To the Graduate Council:

I am submitting herewith a thesis written by John Kenneth Greene entitled "Induction Motor Response During Bus Transfer." I have examined the final copy of this thesis for form and content and recommend that it be accepted in partial fulfillment of the requirements for the degree of Master of Science, with a major in Electrical Engineering.

F. W. Symonds

F. W. Symonds, Major Professor

We have read this thesis
recommend its acceptance:

J M Bailey

J. S. Lawler

Accepted for the Council:

L Evans Roth

Vice Chancellor
Graduate Studies and Research

INDUCTION MOTOR RESPONSE DURING BUS TRANSFER

A Thesis

Presented for the

Master of Science

Degree

The University of Tennessee, Knoxville

John Kenneth Greene

June 1983

1 19[illegible]1

ACKNOWLEDGEMENTS

I am indeed grateful and would like to express my sincere appreciation to B. J. Lamb, Electrical Engineer, for his help in making available a microcomputer compiler, without which the analysis herein would have been extremely proctracted.

I also would like to express my sincere thanks to my advisor, Dr. F. W. Symonds, for his incisive comments, encouragement and guidance, which were essential in the completion of this project.

Finally, I owe special thanks to my wife, Roberta, and sons, George and Robert, for their patience during the research and preparation of this report; and in particular my daughter, Daphne, who typed the draft.

ABSTRACT

The purpose of this study is to examine the electromechanical changes which occur in a three phase induction motor which is connected to a bus with other motors during a bus transfer from one supply to another and thereby predict the likelihood of motor damage to the machine under consideration.

Development of the d-q, two axis model on synchronously rotating axes from the conventional three phase model on stationary axes is presented. This model is then used in the simulation of an auxiliary power system bus in such a manner that the relative rotor flux phase position and magnitude of a single machine may be examined during a bus transfer with the effects of interconnected machines included in the simulation. The program also computes the resultant volts-per-hertz vector between motor and supply at the instant of reclosure to the supply.

This model has been implemented on a microcomputer and the sensitivity of the model to machine data imprecision has been investigated and is reported.

TABLE OF CONTENTS

CHAPTER PAGE

I. INTRODUCTION. 1

II. PROBLEM IDENTIFICATION AND EQUATION DEVELOPMENT . 6
- A. Applicable Industry Standards
- B. Consequences of Excessive Bus Transfer Severity
- C. Induction Motor Origin and General Description
- D. Induction Motor Steady State Equivalent Circuit Model
- E. Development of Complete Induction Motor Model
- F. Development of D-Q Axis Transformation
- G. D-Q Axis Model Steady State Equations
- H. D-Q Axis Models For Two Machine Bus

III. APPLICATION 54
- A. Procedure
- B. Program Development
- C. Motor Data Preperation
- D. Reference Case Study
- E. Motor Data Examination - Case I
- F. Motor Data Examination - Case II

IV. CONCLUSION. 74

LIST OF REFERENCES 76

VITA 78

LIST OF TABLES

TABLE PAGE

3.1. Tabulation of Result Deviations Due to +/- 20 Percent Data Deviation After 9 Cycles For Case I. 61

3.2. Tabulation of Effect of +/- 20 Percent Inertia On Case I 63

3.3. Tabulation Of Effect Of +/- 20 Percent Rotor Resistance on Case I. 65

3.4. Tabulation of Result Deviations Due To +/- 20 Percent Data Deviation After 9 Cycles For Case II. 68

3.5. Tabulation of Effect Of +/- 20 Percent Inertia On Case II. 70

3.6. Tabulation Of Effect Of +/- 20 Percent Rotor Resistance On Case II 72

LIST OF FIGURES

FIGURE		PAGE
1.1.	Typical Auxiliary Power System	2
2.1.	Determination of Resultant Volts/Hertz On Bus transfer or Reclosing.	8
2.2.	Induction Motor	13
2.3.	Magnetic Field Produced In Motor	16
2.4.	Stator MMF.	18
2.5.	Coupled Circuit Representation Of Induction Motor	25
2.6.	Induction Motor Conventional Equivalent Circuit	26
2.7.	Typical Speed Torque Relationship	28
2.8.	Complete Induction Motor Diagram.	30
2.9.	Complete Model Flux Linkage Equation Matrix	31
2.10.	Complete Model Flux Linkage Equation Matrix With Consolidated Inductances	33
2.11.	Three Phase MMF	35
2.12.	Transformation From Fixed A-B Axes To Moving D-Q Axes.	37
2.13.	Development Of [A] Inverse.	39
2.14.	D-Q Axis Transformation Equation Set.	42
2.15.	D-Q Axis Model Equation Set	43
2.16.	Transformed D-Q Axis Model Equations For Short Circuited Rotor	45

FIGURE PAGE

2.17. Induction Motor Steady State Equivalent Circuit Developed From Complete Model 47

2.18. Circulating Current Approach To Solution Of Interconnected Induction Motor Problem. 49

2.19. Two Motor Equation Set For D-Q Model. 50

2.20. Two Motor Equation Set For D-Q Model With D/DT Terms Grouped. 51

2.21. Differential Current Equation Set For D-Q Model 53

3.1. Program Flow Chart. 56

3.2. Plot Of Effect of +/- 20 Percent Inertia on Case I 64

3.3. Plot Of Effect of +/- 20 Percent Rotor Resistance on Case I. 66

3.4. Plot Of Effect of +/- 20 Percent Inertia on Case II. 71

3.5. Plot Of Effect of +/- 20 Percent Rotor Resistance on Case II 73

CHAPTER I

INTRODUCTION

Auxiliary electrical power systems of central generating stations are composed of interconnected load groups called buses which supply mainly induction motor loads which in turn make the electromechanical energy conversion to control mechanical systems which support the turbine-generator and it's auxiliaries. The process of power generation is dependent upon active control of these many mechanical systems which cannot tolerate sustained interruption without causing extensive equipment damage of costly interruption of generation. For this reason, alternate sources of supply are provided for these buses through circuit breakers to transfer the bus from one source to another. Figure 1.1 illustrates a typical electrical auxiliary power system for a single generating unit with buses identified.

As events such as electrical faults, overloads, or maintenance outages occur, transfer of these buses from one source to another is required. Such transfers may be of the:

1. "hot" type where primary and alternate sources are instantaneously paralleled.

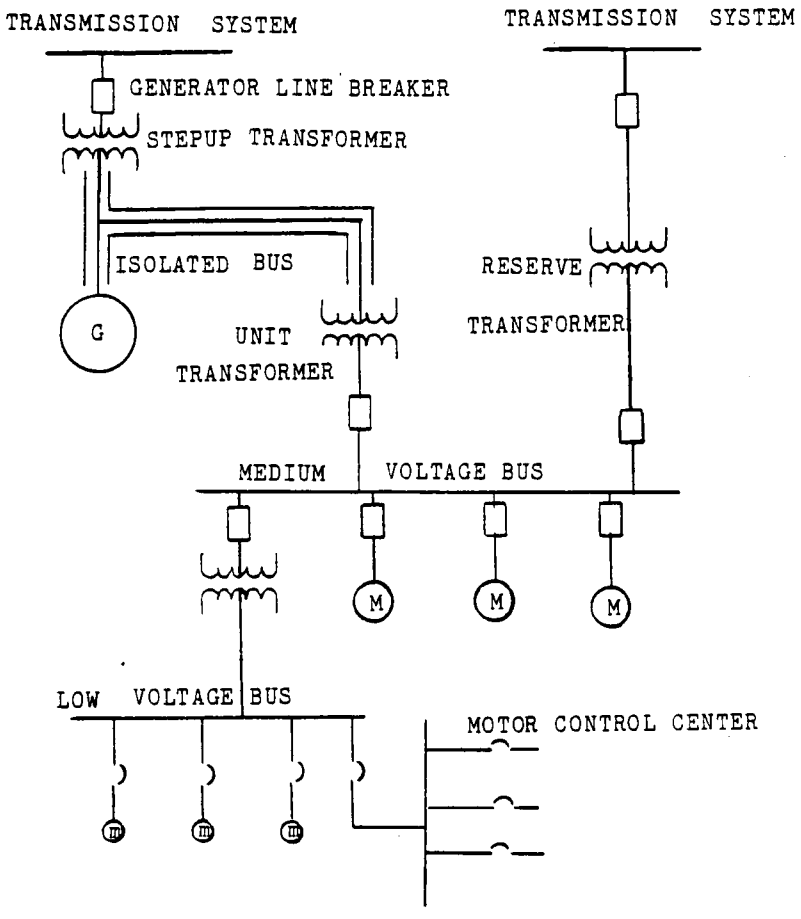


FIGURE 1.1. TYPICAL AUXILIARY POWER SYSTEM

2. "blind" type where closing of an alternate source circuit breaker is initiated simultaneously with initiation of the opening command to the primary source circuit breaker.

3. "fast" type where the closing command to the alternate source breaker is contingent upon at least partial opening of the primary source circuit breaker

4. "delayed" type where closure of the alternate source breaker is restrained until the primary source circuit breaker has opened and the residual voltage of the isolated bus has decayed to a very low value.

The "hot" transfer imposes severe stresses on the electrical auxiliary system, the "blind" transfer has a definite risk of imposing severe stresses on the auxiliary system, the "fast" transfer is relatively safe from the auxiliary power system standpoint, however electromechanical stresses on motors can be significant, and the "delayed" transfer, though safe in regard to both auxiliary power system and motors, can be disruptive to mechanical or fluid systems due to the time delay involved.

Obviously, a means of predicting the severity of electromechanical transients during a "fast" bus transfer of motors connected to the transferred bus would be quite

useful to engineers engaged in designing auxiliary power systems. To be generally useful, such methods must utilize motor data as generally furnished by motor manufacturers, that is, essentially the conventional equivalent circuit parameters. It is the objective of this study to enable prediction of fast bus transfer severity.

The conventional equivalent circuit induction motor model is not accurate for other than steady state operation, hence some form of transient induction motor model is needed. Several such models have been developed, each with associated advantages and disadvantages which will be described in greater detail later. The model selected for this study is the synchronously rotating two axis d-q model claimed by Krause (5). Other authors have also utilized this model (8,9), however their transitions from conventional circuit parameters to model parameters have been obscure, possibly due to limitations in paper length. An additional objective of this study is to illuminate the data manipulation which is necessary to convert conventional equivalent circuit parameters to d-q axis parameters.

Other researchers have studied isolated motors or a composite of all motors on a bus. The limitation of studying an isolated motor is that the effects of other motors on a bus are ignored and conversely, the

disadvantage of a composite motor analysis is that the identity of individual motors is lost and thereby the ability to forecast damage potential for individual motors.

The approach used herein utilized a two motor bus representation, one of which is a particular motor of interest and the other motor is a composite of all other motors on the bus. Hence the effects of a fast bus transfer on a particular motor may be examined with the interaction of interconnected motors taken into consideration. This is a compromise to reduce computational time which would be extremely long if all motors on a bus were discretely modeled.

A final objective of this study was to develop this means of motor bus transfer examination in a form which could be implemented on a personal microcomputer so that it could be widely utilized by practicing engineers. The results of this are reported herein.

CHAPTER II

PROBLEM IDENTIFICATION AND EQUATION DEVELOPMENT

II.A. APPLICABLE INDUSTRY STANDARDS

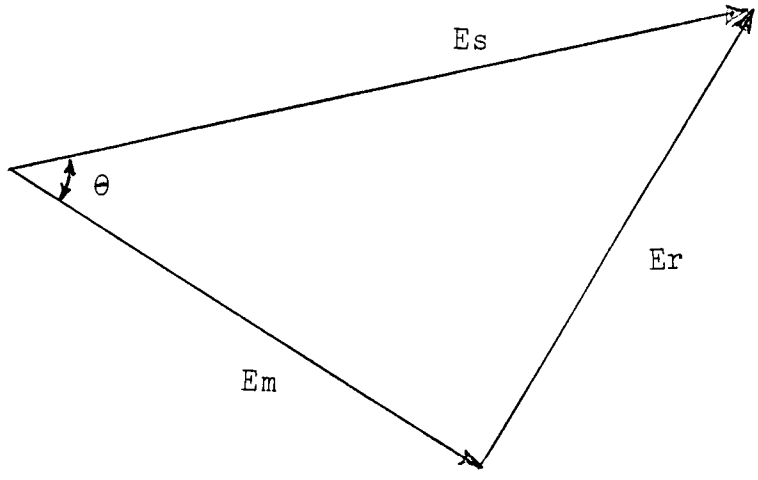
Auxilary power system motors are most commonly of the three phase, single speed, continous duty type and range in voltage from 440 volts to 13600 volts. Horsepower (HP) ratings range from approximately 1 to 12000 or more. These motors in modern installations are built to manufacturers' industry standards contained in NEMA (National Electrical Manufacturers Association) standards identified as MG-1 for smaller motors of under 250 HP and user specifications based on these standards for larger machines. Joint user-manufacturer test standards are contained in the IEEE (Institute of Electrical and Electronic Engineers) Standard 112, "Standard Test Procedure For Polyphase Induction Motors And Generators."

In recognition of the importance of the duty imposed on power generating station auxiliary motors in comparison with other commercial or industrial duty applications a unique standard for motors in these applications, has been developed, which is ANSI (American National Standards Institute) C50.41, "American National Standard For Polyphase Induction Motors For Power

Generating Stations." The aforementioned industry and user standards, with some unique requirements specified in utility procurement documents determine the motor characteristics and data available to utility auxiliary power system designers. They also provide guidance on safe operating limits for motors.

In addition to the more familiar operating limits of voltage, frequency, temperature and load, a limit has been established in ANSI C50.41 governing voltage and phase difference between motors on a transferred bus and the new source during bus transfers. Manufacturers furnishing motors to users specifying this standard are committed to design motors capable of tolerating bus transfers without significant loss of life as long as the resultant vectorial volts per hertz in per unit between the per unit motor residual volts per hertz and the per unit incoming source volts per hertz at the instant the transfer is completed does not exceed 1.33. Conversely utility system designers are expected to effect bus transfers such that this limit is not exceeded. An illustration of this relationship taken from C50.41 is shown in Figure 2.1.

A means of predicting the rotor angle shift of a particular motor during a bus transfer is essential in meeting this criteria from the auxiliary power system



Es = System Equivalent Volts/Hertz In Per Unit

Em = Motor Residual Volts/Hertz In Per Unit

Er = Resultant Vectorial Volts/Hertz in Per Unit

θ = Angle Between Rotor Flux And System Voltage

FIGURE 2.1. DETERMINATION OF RESULTANT VOLTS/HERTZ ON BUS TRANSFER OR RECLOSING

design engineer's viewpoint. A fairly conservative criterion is that the motor rotor change in relative position does not exceed about 90 electrical degrees. This assumes a 30 degree initial difference between rotor flux position and system flux and allows a 60 degree shift in rotor flux axis during the transfer. A more precise measure can be obtained by determining the per unit vectorial resultant volts-per-hertz upon reclosure from;

$$Er/w = \sqrt{(Em/w)^2 + (Es/w)^2 - 2*(Em/w)*(Es/w)*\text{Cos } \theta} \quad (2.1)$$

With frequency change disregarded, motor voltage equal to system voltage and no decay of voltage, the total rotor angle difference from system is 83.5 degrees. The significance of the 1.33 per unit volts-per-hertz limit is that this would have worse case resultant air-gap torque during bus transfer be essentially the same as the torque from a single phase short circuit at the motor terminals.

As described in Chapter I, utlity power system design engineers have used:

1. "Hot" and "blind" transfers to effect motor bus transfers before the relative motor rotor positions could significantly shift;
2. Arbitrary "fast" bus transfer times of 6-8 cycles which experience has shown to be generally satisfactory;

3. Delayed or residual voltage bus transfer to ensure that motor internal voltages have decayed sufficiently to reduce the relative volts-per-hertz ratio to an insignificant value.

The fast bus transfer is a very desireable method from both the power system and process standpoint if it can be accomplished without excessive mechanical or electrical transients. The key to assessing the risks of such a transfer is the relative motor rotor position during a bus transfer. A readily useable means of predicting a particular motor's reaction during a fast bus transfer with other interconnected motors is not readily available to auxiliary power system designers.

II.B. CONSEQUENCES OF EXCESSIVE BUS TRANSFER SEVERITY

At this point, some insight into the consequences of making a fast bus transfer with an excessive volts-per-hertz ratio will underpin the importance of this limitation. An induction motor rotor in normal steady state operation rotates at slightly less than synchronous speed and has a developed magnetic axis locked in with the rotating magnetic axis developed by the stator winding. During a bus transfer, the stator excitation is either removed (as in the case of a single motor) or significantly altered (in the case of interconnected

motors on a bus). Consequently, the motor rotor speed decays as does it's internal voltage. The speed decay introduces an angular difference between the relative rotor magnetic axis and the power system from which primary and alternate sources are obtained. Also, the decay of internal voltage introduces a voltage gradient between the motor and supply sources.

It is conceiveable that during a motor bus transfer, the rotor magnetic axes could shift to a complete reverse polarity while internal voltage is still near normal values. A reconnection to the system at this point could place near twice normal voltage on a saturable device (the motor core) which is normally operated near saturation and extremely high currents would be drawn from the line.

Magnetic forces are related to the current squared, and therefore large forces would be produced in motor windings and mechanical shocks could be inflicted upon the rotor and the shaft connected load; ANSI C50.41 states that values as high as 20 times rated load torque can occur. These can lead to stator winding failures, shaft fatigue and failure or damage to the connected load.

From the power system viewpoint, these high instantaneous currents could cause upstream protective devices to trip and thereby interrupt the alternate source of supply to which a motor or bus is transferred also.

With the overview of a motor bus transfer in mind, a close examination of a three phase induction motor will be made.

II. C. INDUCTION MOTOR ORIGIN AND GENERAL DESCRIPTION

Nicola Telsa first theorized the induction motor in 1888. This electromechanical energy converter changes watts of power into newton-meters of torque via a magnetic field across an air gap between a stationary winding in a magnetic core called a stator and a moving winding on a rotor. This is illustrated in Figure 2.2.

The three phase machine has symmetrically arranged windings which form magnetic pole pairs around a circumferential stator core of laminated steel. These windings are distributed in slots in the core, however in analysis the windings are considered as concentrated turns at the pole axes.

The rotor winding is most commonly of the "squirrel cage" type where rotor conductors form a cylindrical cage which is embedded in the rotor steel body. The rotor is excited from the stator and, when stationary, is equivalent to a transformer with shorted secondary winding. Current flow through the stator winding establishes a magnetic flux in the stator core, most of which crosses the air gap to the rotor.

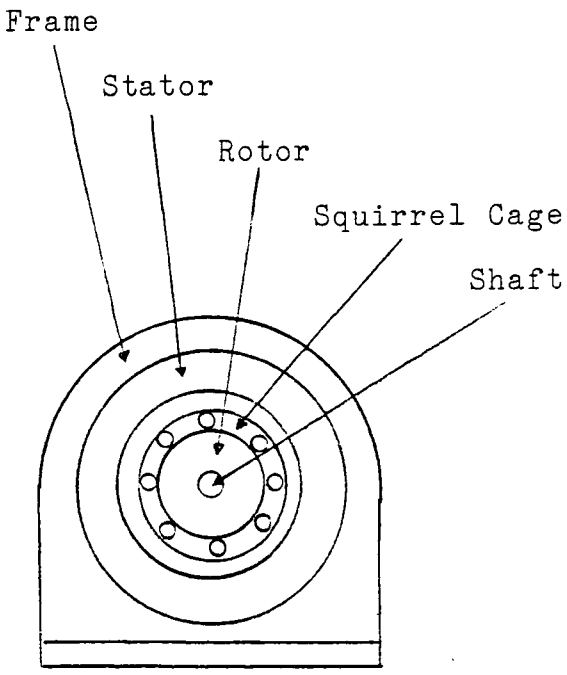


FIGURE 2.2. INDUCTION MOTOR

The flux which does not cross the air gap represents a leakage flux which does not contribute to energy transfer from stator to rotor. The flux crossing the air gap which links stator and rotor windings induces currents in the rotor winding which form magnetic poles which align with the stator poles. The strength of these poles is related to the product of the number of turns of the winding and current flowing through these turns; that is the magnetomotive force (MMF), F.

Once established, the poles of stator and rotor windings will attempt to maintain alignment. The force that attempts to maintain this alignment in a motor is termed torque. The magnitude of this torque is related to the strength of the poles and their relative misalignment. Considering a single phase of a motor winding alone, when at rest, and excited by an alternating current supply, the magnetic pole established by the stator and its companion developed by currents induced in the rotor by transformer action are in phase electrically and spatially. Hence, though the magnetomotive forces may be significant, there is no torque produced which would cause the rotor to move because of the spatial alignment of rotor and stator poles.

The mechanism explaining rotation of the rotor is clearly presented within the "Standard Handbook for Electrical Engineers", (4) and is essentially as follows.

An induction motor with a three phase stator winding spatially distributed around the stator and having 120 degree spatial separation and excited with three phase voltage similarly with electrical phase difference of 120 degrees between phases is considered. An additional constraint is that it is assumed to have a smooth rotor and stator bore, therefore there are no saliency effects.

Considering single full pitch coil of this machine in the stator, and with a uniform air gap between stator and rotor with the effects of slot openings neglected; the field produced by a synchronous voltage on this stator is H=4H/PI(sin X + 1/5 sin 5X +...) which is illustrated in Figure 2.3.

By proper distribution of the winding in the slots and altering the winding pitch, the space harmonics are reduced to negligible value leaving only the fundamental component. The alternating current flowing in the winding of each phase therefore produces an essentially sine wave distribution of magnetic flux around the stator periphery which is stationary in space but varying sinusoidually in magnitude with time in synchronism with supply frequencies.

Now considering the MMF wave of a single phase winding at an angular distance X from the phase axis which can be represented as:

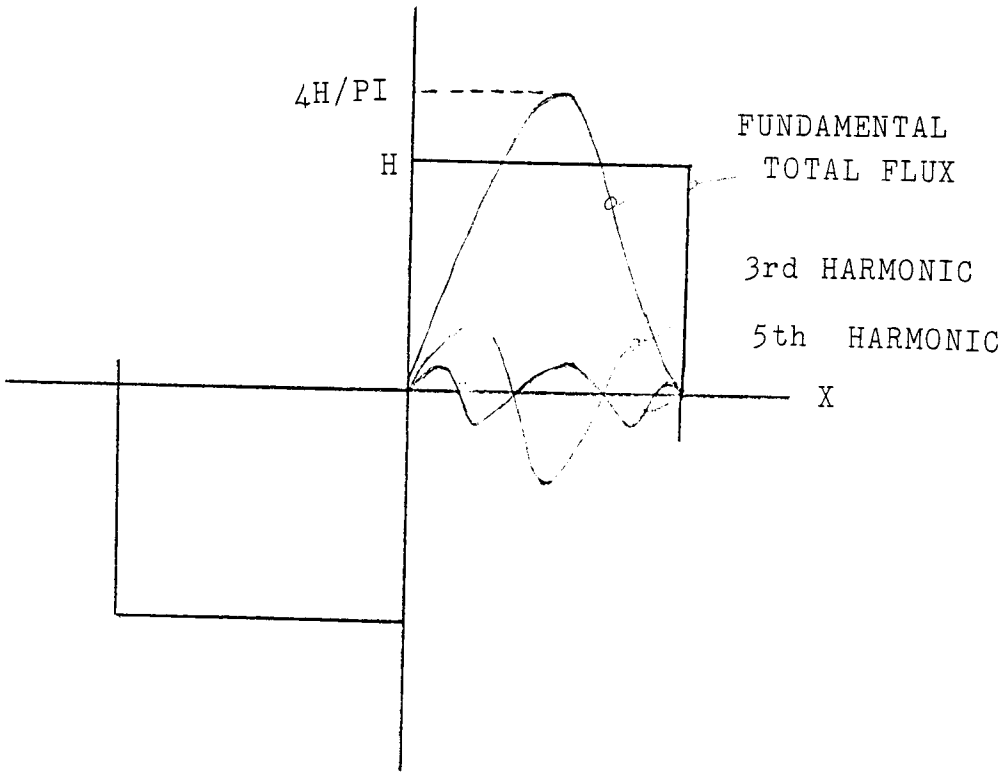


FIGURE 2.3. MAGNETIC FIELD PRODUCED IN MOTOR

$$F * \text{Cos } X * \text{Cos } wT \qquad (2.2)$$

Where X relates the magnitude of MMF, F, to space position and WT relates it to time.

Using the well known trigonometic identity,

$$\text{Cos A Cos B} = 1/2(\text{ Cos (A-B)} + \text{Cos (A+B)}), \qquad (2.3)$$

We may write

$$F \text{ Cos } X \text{ Cos } WT = F*(\text{Cos}(X-WT) + \text{Cos } (X+WT))/2 \qquad (2.4)$$

This can be interpreted as two phasors of equal magnitude revolving in opposite directions at synchronous speed.

Considering phase A alone, see Figure 2.4, the two revolving fields will coincide along the A phase centerline at the instant its current is a maximum. One third of a cycle later, each wave will have traveled 120 electrical degrees, one forward and the other backward, the forward moving wave will line up with the axis of B phase and the backward moving wave will line up with C phase axis.

At this moment, the current in B phase is also a maximum so that the forward-revolving B field is coincident with the forward A field component and these two continue to revolve together. Meanwhile, the backward revolving B field is 240 degrees behind the backward revolving A field and these two remain at this angle as they continue to revolve.

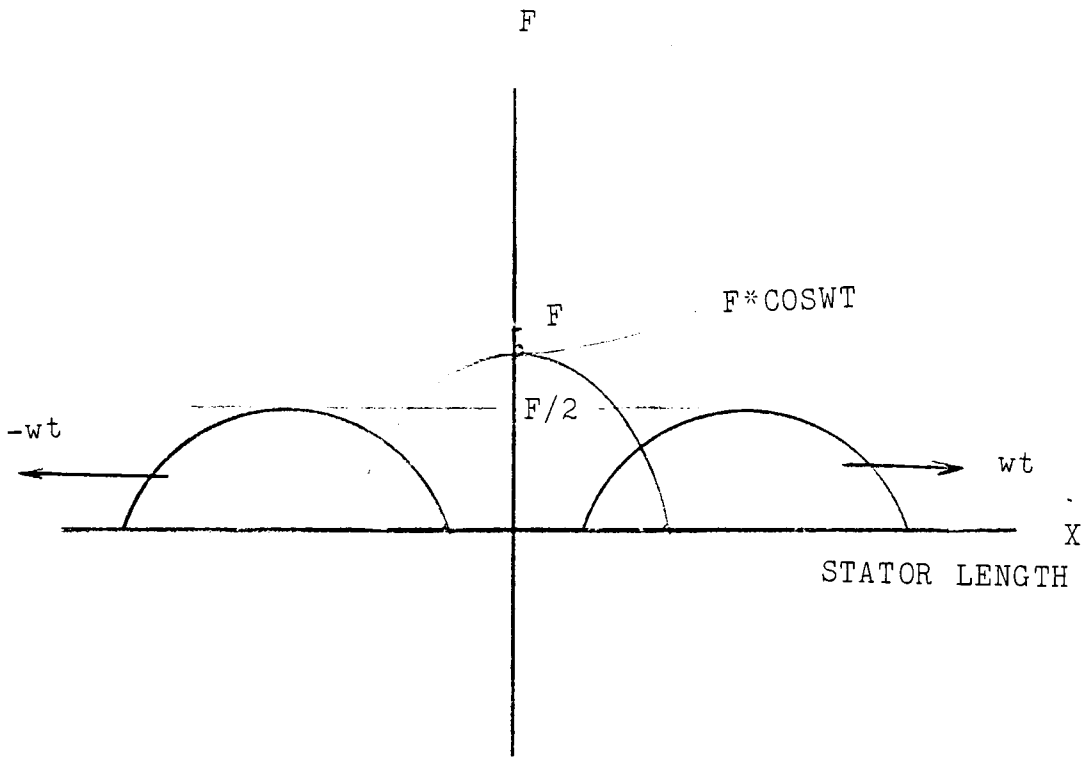


FIGURE 2.4. STATOR MMF

Now after another 1/3 cycle, the forward A and B fields reach the C phase axis at the same moment the phase C current becomes a maximum. Hence, the forward fields of all 3 phases are directly additive, and together they create a constant magnitude sine wave shaped synchronously revolving field with crest value 3/2 times the maximum instantaneous value of the alternating field due to one phase alone. The backward-revolving fields of the 3-phases are separated by 120 degrees and their resultant is therefore zero so long as the 3-phase currents are balanced in both magnitude and phase.

Now the concept of 3-phase excitation of the stator of an induction motor resulting in a synchronously rotating magnetic field in the air gap of 3/2 the magnitude of excitation of a single phase has been established. As this rotating magnetic field "cuts" rotor conductors, voltages are induced in these closed circuits thereby producing currents which flow through the squirrel cage winding producing poles which correspond to the number of poles of the stator. The rotor conductors are arranged in different groups than the stator conductors to preclude direct correspondence of poles and consequent "locking" of the rotor.

With the stator at rest, the induced current in the rotor is at system frequency. The interaction between the flow of current in the squirrel cage conductors and

the air gap flux produces a torque at the rotor surface which is in the direction of rotation of the air gap flux.

The origin of this torque is the local flux density imbalance produced by the flow of current in the rotor conductors. This current flow produces a flux density increase on one side of the conductor and a corresponding flux density decrease on the other side.

The total flux density, which is the summation of the stator flux and the rotor flux, is therefore not uniform in the area of the rotor conductor and the rotor conductor attempts to move into the area of reduced flux density, thereby producing a torque, that is a force at the rotor surface. The torque is maintained as long as the rotating magnetic field and the induced currents exist.

Consequently, the rotor starts rotating in the direction of the rotating field; attempting to line up poles of the rotor with the stator. The rotor speed will always be less than the synchronously rotating flux speed because if there is no relative motion between the conductors on the rotor and the rotating flux wave, no currents will be developed on the rotor, hence no torque will be developed since torque, in essence, is the result of interaction between currents in different windings.

Bear in mind that the force on a current carrying conductor in a magnetic field is $F=Bli * \cos\theta$, where B is

flux density, l is conductor length, i is current and θ is the power factor of the current. For rotor currents to be interactive with air gap flux and produce torque, the rotor power factor angle must not be 90 degrees. A more detailed treatment is done by Nasar and Unnewehr (6).

At standstill the rotor induced currents are at line frequency, at synchronous speed they would be non-existent, that is zero frequency and magnitude. At rotor speeds between zero and synchronous speed, rotor current frequency is at the difference between line frequency and the rotor mechanical speed translated to electrical angular frequency, We, that is mechanical speed, Wm, divided by the number of pairs of electrical poles,N. In equation form,

For the stator: (2.5)

We = Wm / N = 2 * PI * Line Frequency / Pole Pairs

For the rotor: (2.6)

Wm - We = 2 * PI * Rotor Frequency / Pole Pairs

where Rotor frequency= Line Frequency * Slip of rotor with respect to revolving field of stator

As with the three phase stator currents, these three phase rotor currents develop a concentrated magnetomotive force which travels in advance of the rotor at a speed of Slip * We(stator) and since the rotor is traveling at a speed of (1-Slip)*We(stator), the speed of the rotor flux wave in relation to the stator is Slip *

We(stator) + (1-Slip) * We(stator) = We(stator). Thus the rotor and stator traveling flux waves for a three phase machine are in alignment and the force keeping them in alignment:

1. Is dependent on the rotor pole strength which
2. Is dependent on the rotor current which
3. Is dependent on voltage induced in the rotor which
4. Is dependent on a stator induced flux sweeping past closed circuited rotor conductors which
5. Is dependent on relative difference in angular speed between stator flux and the rotor.

The greater the difference between the rotor velocity and the stator flux angular velocity, the greater will be the induced rotor voltage, hence the greater the rotor current and consequently the rotor pole strength. The increased rotor current increases local flux density imbalance at the rotor surface and consequently the torque. At standstill, the rotor slip is highly reactive due to the large slip, and consequent large rotor current frequency, and torque the is thereby limited. As the rotor speed increases, and the slip decreases, the rotor current frequency drops as does its reactance and power factor angle, thereby increasing torque to near the point where inductive reactance is equal to rotor resistance, that is the maximum power transfer point. In this region,

torque is limited by reduced rotor current which at synchronous speed is zero and produces no torque.

II.D. INDUCTION MOTOR STEADY STATE EQUIVALENT CIRCUIT MODEL

Now a mathematical model to relate the aforementioned interactive elements in steady state, that is constant speed operation, is presented. The portion of stator flux which does not link the rotor does not perform useful work and is termed leakage flux symbolized by an inductance element Ls. Similarly there is some rotor flux which does not link the stator which is wasted and will be symbolized by the inductance element Lr. The portion of flux which links both rotor and stator, through which power is transferred across the motor air gap is called mutual flux and is represented by the term Lm. Recall that inductances, L, are those derived constants relating voltages to the rate of change of flux linkages, that is

$$E=-L * dF/dt=-L* N * di/dt \qquad (2.7)$$

Where F = N * I in ampere-turns.

There are also resistive losses in the stator conductors which are represented by Rs and the rotor conductors in the form of Rr. Losses exist in the mutually coupled branch in the form of eddy and hysterises losses in the magnetic materials but those are usually ignored because of their small magnitude.

Integrating these parameters, we obtain a coupled circuit as shown in Figure 2.5 wherein the term "s" is the percent slip of the rotor with respect to the synchronously rotating stator field.

With rotor quantities referred to the stator, this becomes as shown in Figure 2.6 for steady state operation.

This is the conventional equivalent circuit induction motor model. It is in this form that motor parameters are supplied from motor manufacturers to users. Data for this model is obtained from standardized tests. This data is normally provided on a "per phase" basis, thus three phase performance is obtained by multiplying single phase results by 3. The term Rr/s in the rotor branch when multiplied by the current in that branch squared represents power converted into torque.

An analysis of this model results in the following expression for power crossing the air gap which is available for conversion into torque:

$$\text{Power / phase} = (Rr * Ir^2)/s = \qquad (2.8)$$

$$\frac{(Rr/s)\ [Xm\,V]^2}{\left[Rr*(Rr/s) - (XsXm+XsXr+XmXr)\right]^2 + \left[(Rr(Xr+Xm)/s) + Rs(Xm+Xr)\right]^2}$$

Torque is equal to power divided by mechanical speed, hence

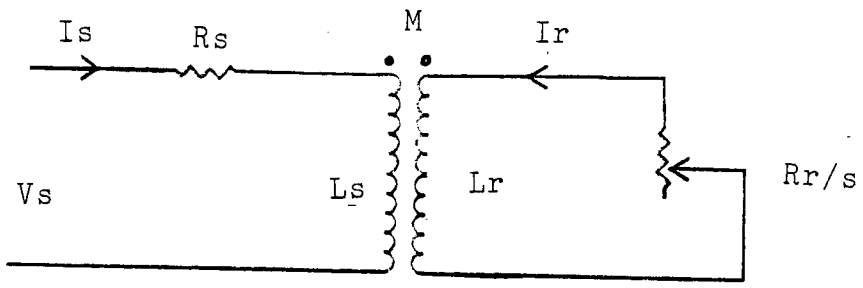


FIGURE 2.5. COUPLED CIRCUIT REPRESENTATION OF INDUCTION MOTOR

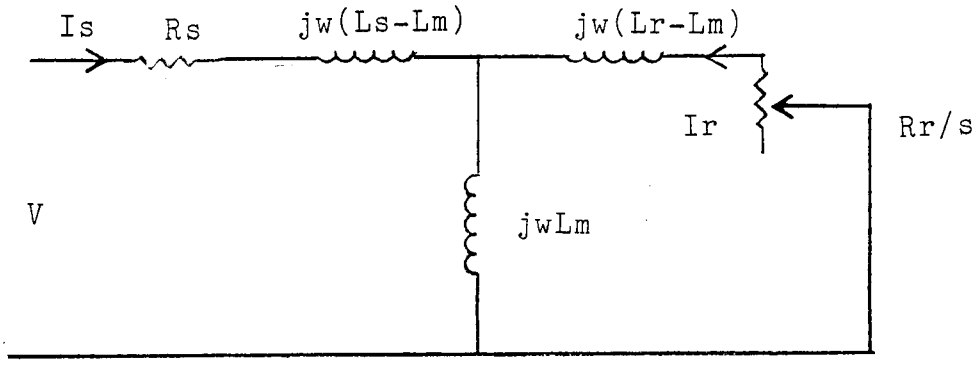


FIGURE 2.6. INDUCTION MOTOR CONVENTIONAL EQUIVALENT CIRCUIT

$$\text{Torque / phase} = \text{Power / phase} * W_m \qquad (2.9)$$

$$= \text{Power / phase} * W_e / \text{Pole Pairs}$$

$$= (\text{Power / \# phase}) * (\text{Pole Pairs} / W_e)$$

From this expression, the familiar speed-torque curve of an induction motor is developed. As slip is varied, a relationship to torque such as depicted in Figure 2.7 results. The peak of the curve, or breakdown torque point, is near the point at which rotor reactance and rotor resistance are equal.

The normal operating region of a motor is between the speed corresponding to breakdown torque and synchronous speed. Increasing load results in increased slip which, in this reqion, results in increased torque.

As stated previously, this model describes constant speed operation and does not represent time varying inductances which relative motion between rotor and stator windings inherently develop. Therefore, it cannot model transient conditions which would certainly be influenced by these time varying quantities.

To analyze transient conditions, the effect of time varying inductances must by included. To do this a complete model of an induction motor is presented from which the aforementioned steady state representation can be developed.

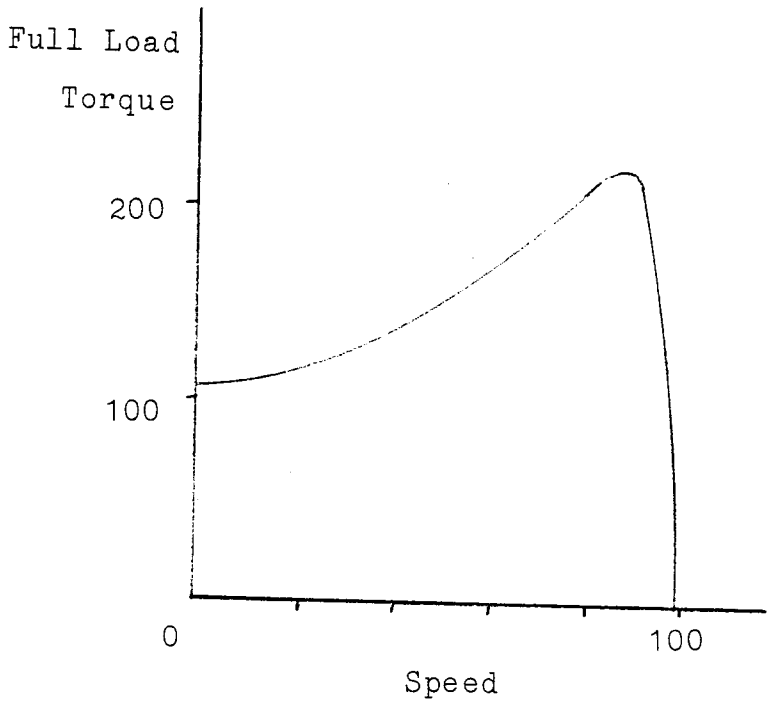


FIGURE 2.7. TYPICAL SPEED TORQUE RELATIONSHIP

II.E. DEVELOPMENT OF COMPLETE INDUCTION MOTOR MODEL

The basis for this development is depicted in Figure 2.8, from which an equation set is written for a cylindrical rotor two pole induction motor in balanced three phase operation.

The basic voltage equation applicable to this circuit is $V = p\lambda + R*I$ where is the total flux linkages, R is the winding resistance and p is the operator d/dt. Writing these expressions for each winding we obtain:

$$\begin{aligned} Vas &= p\lambda as + R * Ias \\ Vbs &= p\lambda bs + R * Ibs \\ Vcs &= p\lambda cs + R * Ics \\ Var &= p\lambda ar + R * Iar \\ Vbr &= p\lambda br + R * Ibr \\ Vcr &= p\lambda cr + R * Icr \end{aligned} \qquad (2.10)$$

Expanding this into the total flux linkage for each phase and, using matrix notation, noting that $[\lambda] = [L]\ [I]$, the equation set illustrated in Figure 2.9 is written.

Note that in this expression, the terms involving mutual inductance between stator and rotor are dependent upon the rotor angle, θ, while other inductances are independent of it. Consider the equation for the "a" phase flux linkages,

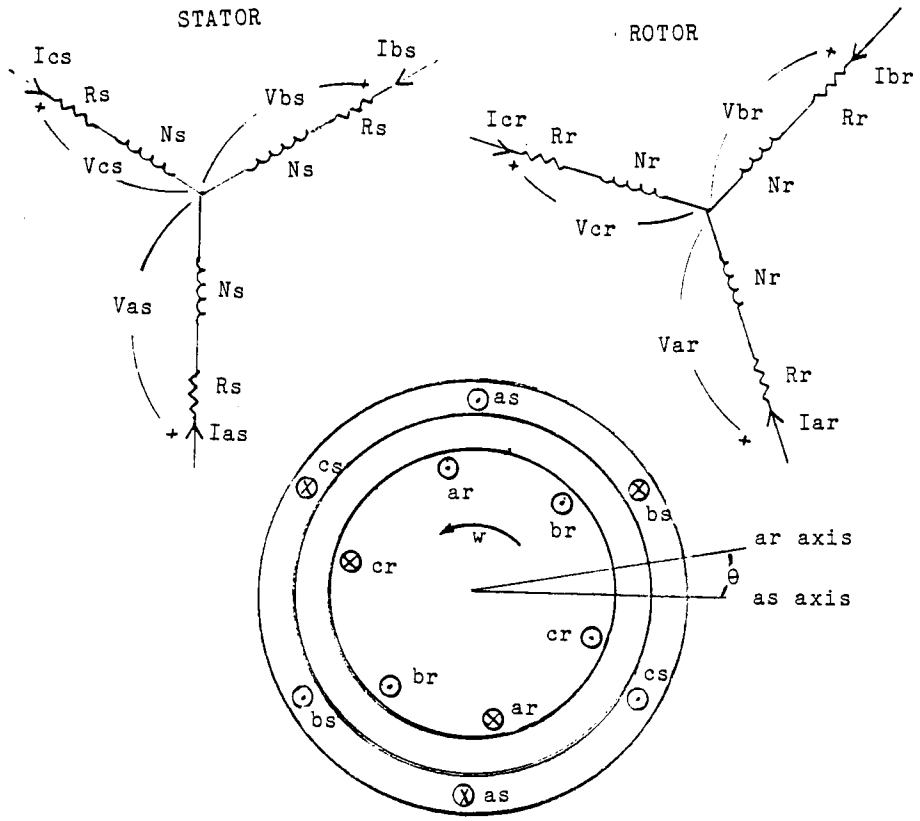


FIGURE 2.8. COMPLETE INDUCTION MOTOR DIAGRAM

$$
\begin{bmatrix} \lambda as \\ \lambda bs \\ \lambda cs \\ \lambda ar \\ \lambda br \\ \lambda cr \end{bmatrix} = \begin{bmatrix} Ls & Ms & Ms & MsrCos\theta & MsrCos(\theta+120) & MsrCos(\theta-120) \\ Ms & Ls & Ms & MsrCos(\theta-120) & MsrCos\theta & MsrCos(\theta+120) \\ Ms & Ms & Ls & MsrCos(\theta+120) & MsrCos(\theta-120) & MsrCos\theta \\ MsrCos\theta & MsrCos(\theta-120) & MsrCos(\theta+120) & Lr & Mr & Mr \\ MsrCos(\theta+120) & MsrCos\theta & MsrCos(\theta-120) & Mr & Lr & Mr \\ MsrCos(\theta-120) & MsrCos(\theta+120) & MsrCos\theta & Mr & Mr & Lr \end{bmatrix} \begin{bmatrix} Ias \\ Ibs \\ Ics \\ Iar \\ Ibr \\ Icr \end{bmatrix}
$$

where Ls = stator self inductance per phase

Ms = mutual inductance linking one stator phase with other stator phases

Msr= Mutual inductance linking one stator phase with one rotor phase

Mr = mutual inductance linking one rotor phase with other rotor phases

Lr = rotor self inductance per phase

FIGURE 2.9 COMPLETE MODEL FLUX LINKAGE EQUATION MATRIX

$$\lambda as = Ls * Ias + Ms*(Ibs + Ics) + \quad (2.11)$$

$$Msr(IarCos\theta + IbrCos(\theta-120) + IcrCos(\theta+120))$$

For three phase balanced operation, which we have specified as the basis of this invesitgation, the relationship between phase currents is;

$$Ias + Ibs + Ics = 0$$

Therefore

$$Ias = -(Ibs + Ics) \quad (2.12)$$

And

$\lambda as = (Ls-Ms)Ias + Msr(IarCos\theta + IrbCos(\theta+120) + IcrCos(\theta-120))$

The other rotor only and stator only flux linkage expressions are similarly manipulated and the resulting flux linkages expressed in matrix form are as shown in Figure 2.10.

At this juncture, development of the desired induction motor model may proceed with time varying mutual inductance terms such as described by Daugherty (2), or expedient transformations of the reference axes may be utilized to simplify analysis and computations.

Such a transformation which aids induction motor analysis is one wherein the stationary three phase quantities are transformed into synchronously two phase quantities on orthogonal axes. Likewise the three phase rotor quantities which rotate at less than synchronous

$$
\begin{bmatrix} \lambda as \\ \lambda bs \\ \lambda cs \\ \lambda ar \\ \lambda br \\ \lambda cr \end{bmatrix} =
\begin{bmatrix}
Ls-Ms & 0 & 0 & MsrCos\theta & MsrCos(\theta+120) & MsrCos(\theta-120) \\
0 & Ls-Ms & 0 & MsrCos(\theta-120) & MsrCos\theta & MsrCos(\theta+120) \\
0 & 0 & Ls-Ms & MsrCos(\theta+120) & MsrCos(\theta-120) & MsrCos\theta \\
MsrCos\theta & MsrCos(\theta-120) & MsrCos(\theta+120) & Lr-Mr & 0 & 0 \\
MsrCos(\theta+120) & MsrCos\theta & MsrCos(\theta-120) & 0 & Lr-Mr & 0 \\
MsrCos(\theta-120) & MsrCos(\theta+120) & MsrCos\theta & 0 & 0 & Lr-Mr
\end{bmatrix}
\begin{bmatrix} Ias \\ Ibs \\ Ics \\ Iar \\ Ibr \\ Icr \end{bmatrix}
$$

FIGURE 2.10. COMPLETE MODEL FLUX LINKAGE EQUATION MATRIX WITH CONSOLIDATED INDUCTANCES

speed are transformed to these same synchronously rotating orthogonal axes. This is the "d-q" transformation with synchronously rotating axes as reported by Krause in reference(5).

II.F. DEVELOPMENT OF D-Q AXIS TRANSFORMATION

The transformation from a-b-c three phase axes to rotating d-q two phase axes is most clearly approached via an intervening transformation to stationary two phase A-B axes as is done by O'Kelley and Simmons (7) for stator fixed axes. Bear in mind that for the sought transformation to be valid, the instantaneous flux in the two phase transformed system must be equal to the flux developed in the original system. This is because the flux is that medium through which electrical energy is converted to mechanical energy.

Consider the flux portrayals in Figure 2.11. The equations relating fixed three phase axes and fixed two phase axes are;

$$FA = Fa + FbCos\ 120 + FcCos(-120)$$

Hence, $FA = Fa - (Fb / 2) - (Fc / 2)$

And $FB = Fb\ Sin(120) + Fc\ Sin(-120)$

Hence, $FB = \sqrt{3}\ Fb/2 - \sqrt{3}\ Fc/2$ (2.14)

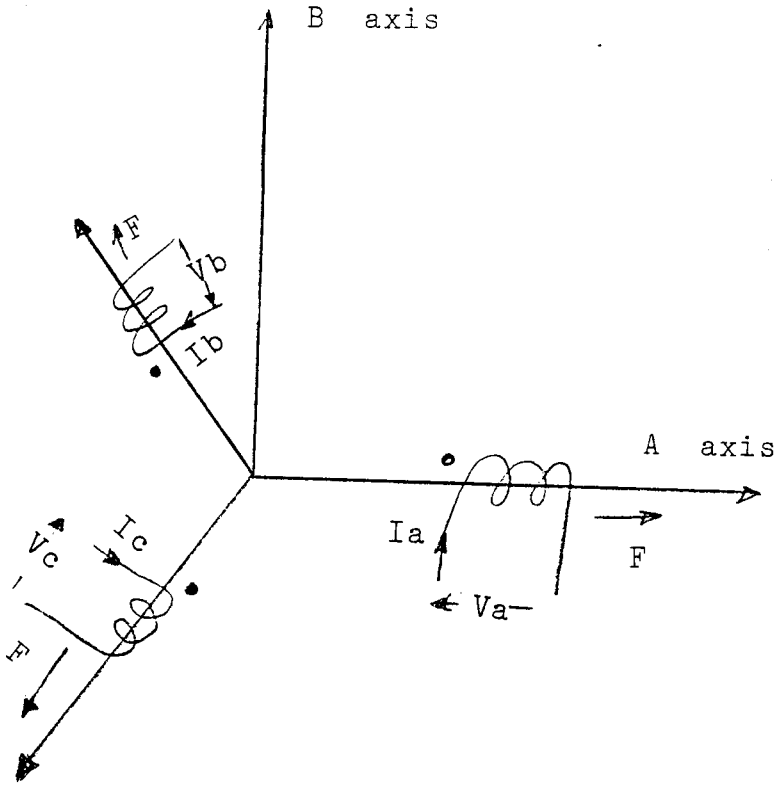


FIGURE 2.11. THREE PHASE MMF

Or in matrix form,

$$[FA,B]^t = \begin{bmatrix} 1 & -1/2 & -1/2 \\ 0 & /3/2 & -/3/2 \end{bmatrix} [Fa,b,c]^t$$

These expressions describe the flux created by a three wire, three phase system or a balanced four wire system. If unbalanced systems are considered, a third equation is required. Unbalanced systems are not treated in this study and this third equation is not needed, however, it is expedient to form a square matrice which can readily be manipulated. To accomplish this, the flux which would be created by a neutral current is arbitrarily selected to be;

$$Fo = k * (Fa + Fb + Fc) \qquad (2.14)$$

Thus we have in matrice form;

$$[FA,B,O]^t = \begin{bmatrix} 1 & -1/2 & -1/2 \\ 0 & /3/2 & -/3/2 \\ k & k & k \end{bmatrix} [Fa,b,c]^t \qquad (2.15)$$

With rotation of the d-q axes in relation to the A-B axes considered as illustrated in Figure 2.12, the following expression for the transformation is obtained;

$$[Fq,d,o]^t = \begin{bmatrix} FACos0 & FBSin0 & 0 \\ FASin0 & -FBCos0 & 0 \\ 0 & 0 & FO \end{bmatrix} =$$

$$= \begin{bmatrix} Cos0 & Sin0 & 0 \\ Sin0 & -Cos0 & 0 \\ 0 & 0 & 1 \end{bmatrix} \begin{bmatrix} FA \\ FB \\ FO \end{bmatrix}$$

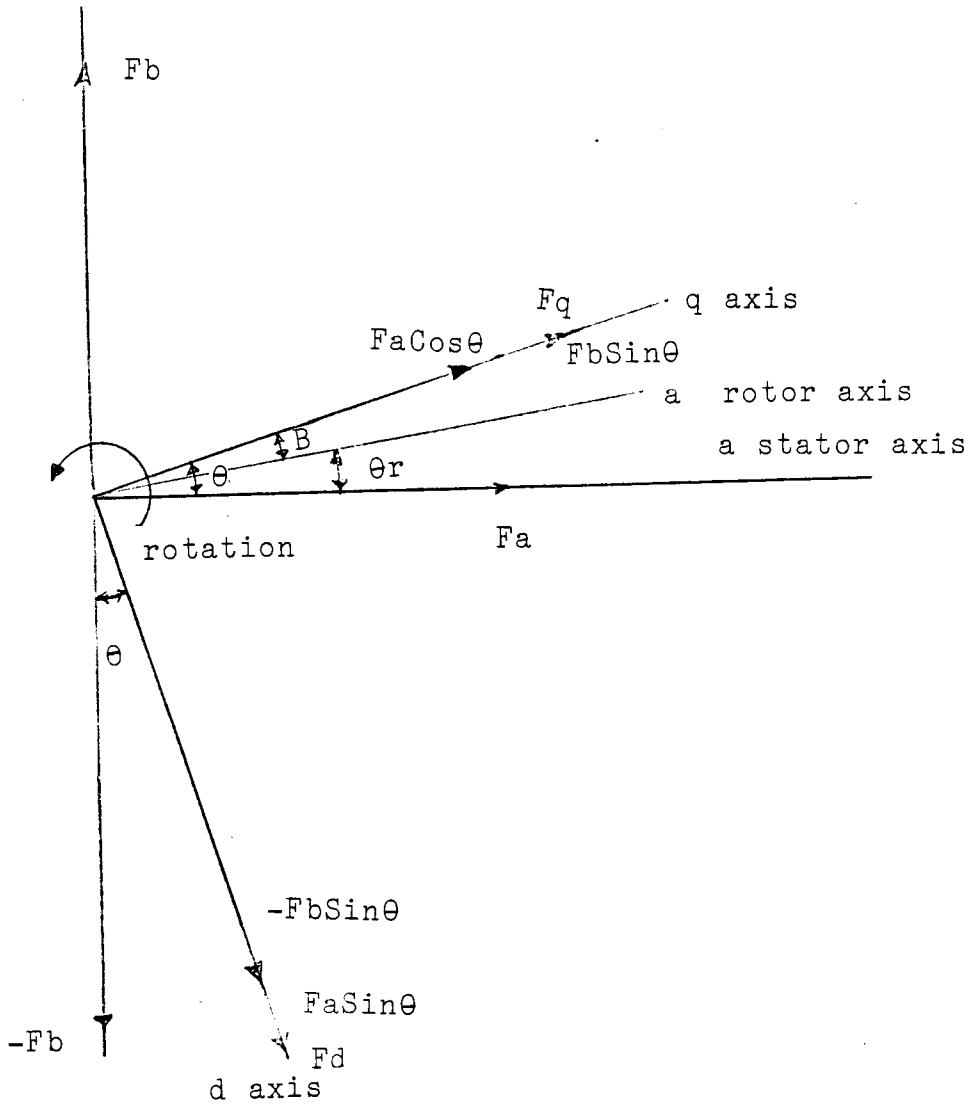


FIGURE 2.12. TRANSFORMATION FROM FIXED A-B AXES TO MOVING D-Q AXES

To complete the transition from [Fa,b,c] to [Fq,d,o] the two transformations derived thus far are combined as follows;

$$\left[Fq,d,o\right] = {}^{t}\begin{bmatrix} \mathrm{Cos}\theta & \mathrm{Sin}\theta & 0 \\ \mathrm{Sin}\theta & -\mathrm{Cos}\theta & 0 \\ 0 & 0 & 1 \end{bmatrix}\begin{bmatrix} 1 & -1/2 & -1/2 \\ 0 & /3/2 & -/3/2 \\ k & k & k \end{bmatrix}\begin{bmatrix} Fa \\ Fb \\ Fc \end{bmatrix} =$$

$$\begin{bmatrix} \mathrm{Cos}\theta & (-\mathrm{Cos}\theta + \sqrt{3}\mathrm{Sin}\theta)/2 & (-\mathrm{Cos}\theta - \sqrt{3}\mathrm{Sin}\theta)/2 \\ \mathrm{Sin}\theta & (-\mathrm{Sin}\theta - \sqrt{3}\mathrm{Cos}\theta)/2 & (-\mathrm{Sin}\theta + \sqrt{3}\mathrm{Cos}\theta)/2 \\ k & k & k \end{bmatrix}\begin{bmatrix} Fa \\ Fb \\ Fc \end{bmatrix} \tag{2.17}$$

$$\begin{bmatrix} \mathrm{Cos}\theta & (\mathrm{Cos}\theta\mathrm{Cos}120+\mathrm{Sin}\theta\mathrm{Sin}120) & (\mathrm{Cos}\theta\mathrm{Cos}240+\mathrm{Sin}\theta\mathrm{Sin}240) \\ \mathrm{Sin}\theta & (\mathrm{Sin}\theta\mathrm{Cos}120-\mathrm{Cos}\theta\mathrm{Sin}120) & (\mathrm{Sin}\theta\mathrm{Cos}240-\mathrm{Cos}\theta\mathrm{sin}240) \\ k & k & k \end{bmatrix}\begin{bmatrix} Fa \\ Fb \\ Fc \end{bmatrix}$$

Then using trigonometric identities

$$\mathrm{Cos}(x+/-y) = \mathrm{Cos}x\mathrm{Cos}y \; -/+ \; \mathrm{Sin}x\mathrm{Sin}y \tag{2.18}$$

$$\mathrm{Sin}(x+/-y) = \mathrm{Sin}x\mathrm{Cos}y \; +/- \; \mathrm{Cos}x\mathrm{Sin}y$$

The following result is obtained;

$$\left[Fd,q,o\right] = {}^{t}\begin{bmatrix} \mathrm{Cos}\theta & \mathrm{Cos}(\theta-120) & \mathrm{Cos}(\theta+120) \\ \mathrm{Sin}\theta & \mathrm{Sin}(\theta-120) & \mathrm{Sin}(\theta+120) \\ k & k & k \end{bmatrix}\begin{bmatrix} Fa \\ Fb \\ Fc \end{bmatrix} =$$

$$= \left[A\right]\left[Fa,b,c\right] \tag{2.19}$$

The development of the expression for the inverse transformation is similiar and is as shown in Figure 2.13.

Thus the transformation and it's inverse from a,b,c three phase stationary axes to q,d,o synchronously

$$[A]\ \text{inverse} = [A]\ \text{cofactor, transpose}$$

$$= \frac{\begin{matrix} k(\text{Sin}(\theta-120) - \text{Sin}(\theta+120)) & -k(\text{Sin}\theta - \text{Sin}(\theta+120)) & k(\text{Sin}\theta - \text{Sin}(\theta-120)) \\ -k(\text{Cos}(\theta-120) - \text{Cos}(\theta+120)) & k(\text{Cos}\theta - \text{Cos}(\theta+120)) & -k(\text{Cos}\theta - \text{Cos}(\theta-120)) \\ k(\text{Cos}\theta-120)\text{Sin}(\theta-120) - & -k(\text{Cos}\theta\text{Sin}(\theta+120) - & k(\text{Cos}\theta\text{Sin}(\theta-120) - \\ \text{Cos}(\theta+120)\text{Sin}(\theta-120)) & \text{Cos}(\theta+120)\text{Sin}\theta) & \text{Cos}(\theta-120)\text{Sin}\theta) \end{matrix}}{k\text{Cos}\theta(\text{Sin}(\theta-120)-\text{Sin}(\theta+120)) - k\text{Sin}\theta(\text{Cos}(\theta-120)-\text{Cos}(\theta+120)) + k(\text{Cos}\theta-120)\text{Sin}(\theta+120) - \text{Cos}(\theta+120)\text{Sin}(\theta-120))}$$

$$[A]\ \text{inverse} = (2/3) \begin{bmatrix} \text{Cos}\theta & \text{Sin}\theta & -1/2k \\ \text{Cos}(\theta-120) & \text{Sin}(\theta-120) & -1/2k \\ \text{Cos}(\theta+120) & \text{Sin}(\theta+120) & -1/2k \end{bmatrix}$$

FIGURE 2.13 DEVELOPMENT OF [A] INVERSE

rotating axes for MMF has been demonstrated. In the development of subsequent transformations for currents, the choice of the turns ratio between the coils of the originial a-b-c three phase model and the coils of the q-d-o two phase model is completely arbitrary and the choice of the constant k in the transformation matrix is also arbitrary as long as only balanced operation is considered.

The selection of these two constants will introduce or surpress constants in subsequently derived transformations for currents, voltages and inductances. The procedure followed in developing these other transformations is next to develop a transformation for currents from the previously developed expression for the MMF, which is equal to the ampere-turns in the coil model under consideration.

In equation form,

$$[Fa,b,c] = N1\,[Ia,b,c] \qquad (2.20)$$

And,

$$[Fq,d,o] = N2\,[Iq,d,o] \qquad (2.21)$$

From which we obtain;

$$[Ia,b,c] = [Fa,b,c] \;/\; N1 \qquad (2.22)$$

And

$$[Iq,d,o] = [Fq,d,o] \;/N2 = [A]\;[Fa,b,c] \;/N2$$
$$= (N1/N2) * [A]\;[Ia,b,c] \qquad (2.23)$$

With the current transformation developed, the voltage transformation is developed within the constraint of power invariance. This is necessary to insure that torques and losses in the two models agree. Power invariance in equation form is;

$$[V_{a,b,c}]\ [I_{a,b,c}] = [V_{q,d,o}]\ [I_{q,d,o}] \qquad (2.24)$$

Next the transformation for the machine resistances and inductances are developed from the previously derived voltage and current relationships which in matrix form are;

$$[V_{a,b,c}] = [Z_{a,b,c}]\ [I_{a,b,c}] \qquad (2.25)$$

And

$$[V_{q,d,o}] = [Z_{a,b,c}]\ [I_{q,d,o}] \qquad (2.26)$$

These manipulations are quite tedious and results have been reported for optimum choices of turns ratios and arbitrary constants by Krause (5). The transformation equations which are valid for currents and voltages are shown in Figure 2.14.

From the previous development, it can be seen that k=1/3 and N1/N2 = 2/3.

This transformation to the d-q axes replaces both the rotor and stator variables with transformed variables such that the transformed equations no longer explicitly contain the rotor angle, O. Instead, a speed dependent term, dO/dt (which is W), is introduced. The equation set for this model in matrix form is shown in Figure 2.15.

$$fqs = (2/3)\,(fasCos\theta + fbsCos(\theta-120) + fcsCos(\theta+120))$$

$$fds = (2/3)\,(fasSin\theta + fbsSin(\theta-120) + fcsSin(\theta+120))$$

$$fos = (1/3)\,(fas + fbs + fcs)$$

$$fqr = (2/3)\,(farCosB + fbrCos(B-120) + fcrCos(B+120))$$

$$fdr = (2/3)\,(farSinB + fbrSin(B-120) + fcrSin(B+120))$$

$$for = (1/3)\,(far + fbr + fcr)$$

FIGURE 2.14 D-Q AXIS TRANSFORMATION EQUATION SET

$$\begin{bmatrix} Vds \\ Vqs \\ Vdr \\ Vqr \end{bmatrix} = \begin{bmatrix} Rs+pLs & wLs & pM & wM \\ -wLs & Rs+pLs & -wM & pM \\ pM & SwM & Rr+pLr & SwLr \\ -SwM & pM & -SwLr & Rr+pLr \end{bmatrix} \begin{bmatrix} Ids \\ Iqs \\ Idr \\ Iqr \end{bmatrix}$$

WHERE

s and r refer to stator and rotor quantities

d and q refer to direct and quadrature axes

Rs = Stator resistance per phase

Rr = Rotor Resistance per phase

M = (3/2) Mutual inductance per phase

Ls = Stator leakage plus mutual inductance

Lr = Rotor Leakage plus mutual inductance

w = Synchronous speed

S = Slip of rotor with respect to w

p = Differential operator, d/dt

FIGURE 2.15 D-Q AXIS MODEL EQUATION SET

The torque expression for this model is,

$$Te = (phases/2) * (Poles/2) * M * (IqsIdr - IdsIqr) \quad (2.27)$$

Where the last term is the net effect of stator and rotor currents.

From which the complete electromechanical torque, Tm, equation is,

$$J\,p(Wm) + A(Wm) + Tm = Te \quad (2.28)$$

Where

J = inertia

A = viscous damping coeffecient

Wm = mechanical speed in radians per second

Tm = Load torque in newton-meters

II.G. D-Q AXIS MODEL STEADY STATE EQUATIONS

Now following the development described by Shastry and Burridge (9), the d-q axis model equations for synchronously rotating axes with shortcircuited rotor and no initial phase difference between the rotor and phase axes is compactly written in matrix form as shown in Figure 2.16.

The steady state version of this model is formed by manipulation of the equations to produce phasor quantities, that is,

$$\begin{bmatrix} V \\ 0 \\ 0 \\ 0 \end{bmatrix} = \begin{bmatrix} Rs+pLs & -wLs & pM & -wM & 0 \\ wLs & Rs+pLs & wM & pM & 0 \\ pM & -SwM & Rr+pLr & -SwLr & 0 \\ SwM & pM & SwLr & Rr+pLr & 0 \end{bmatrix} \begin{bmatrix} Ids \\ Iqs \\ Idr \\ Iqr \end{bmatrix}$$

$$[T] = [nMIqr \quad -nMIrd \quad 0 \quad 0 \quad (Jp+A)/n] \quad [w]$$

WHERE previously undefined terms are

n = Number of phases

J = Inertia

A = Viscous Damping Coeffecient

T = Electromagnetic torque

FIGURE 2.16 TRANSFORMED D-Q AXIS MODEL EQUATIONS FOR SHORT CIRCUITED ROTOR

Multiply row 2 by j and add to row 1, yielding

$$V = (Isd+jIsq)(Rs+jwLs)+Ls(pIsd+jpIsq) + E$$

where (2.29)

$$E=((Isd+Ird)+j(Isq+Irq))jwM + pM((Isd+Ird)+j(Isq+Ird))$$

And similiarly for rows 3 and 4 with $(w-Wr)=s*W$,

$$0=(Ird+jIrq)(Rr/s + Jwlr)+pLr(Ird+jIrq)/s + E +$$

$$M(1-s)p((Isd+Ird) + j(Isq+Irq))/s \quad (2.30)$$

Now set $d/dt = 0$, hence $p = 0$ and (2.31)

$$V = (Isd+jIrq)(Rs+jwLs) + jwM((Isd+Ird)+j(Isq+Irq))$$

And (2.32)

$$0 = (Ird+jIrq)(Rr/s + jwLr)+JwM((Isd+Ird)+jIsq+Irq))$$

These equations represent an equivalent circuit as portrayed in Figure 2.17.

Manipulating these equations algebraically yields the following expressions for model currents which are suitable for implementation on a digitial computer to obtain steady state operating parameters,

$$Isd =(V+wM(Irq-wLsIrd/Rs)/D \quad (2.33)$$

$$Isq = -(wMIrd+wLs(V+wMIrq)/Rs)/D$$

$$Ird = (B1*V1^2 - B2*V2)/(B1^2 + B2^2)$$

$$Irq = (B2*V1^2 + B1*V2)/(B1^2 + B2^2)$$

Where

$A11 = (Lr-w^2*M^2*Ls)/(Rs+D)$

$A12 = w*M^2 / D$

$S = slip$

$V2 = V*M*s*w/D$

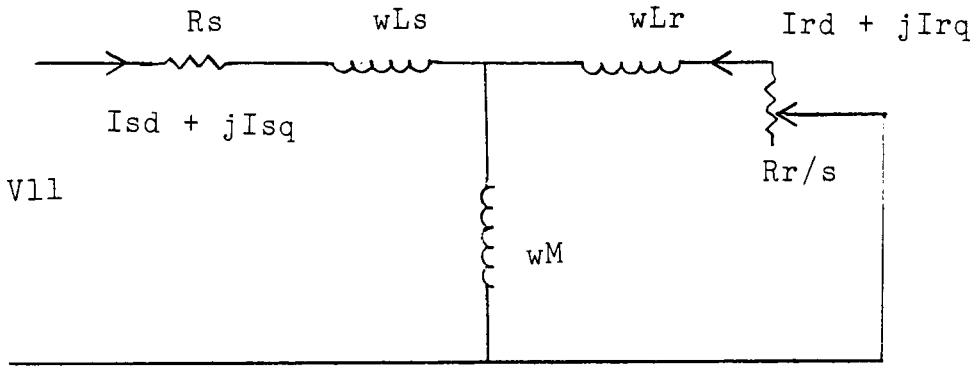


FIGURE 2.17. INDUCTION MOTOR STEADY STATE EQUIVALENT CIRCUIT DEVELOPED FROM COMPLETE MODEL

V1 =V2*w*Ls / Rs

D =(Rs^2 + w^2*Ls^2) / Rs

B1 =-(Rr +A12 * s * w)

B2 =A11 * s * w

The associated torque expression for digitial solution is;

Te = N*M*(IsqIrd - IsdIrq) (2.34)

II.H. D-Q AXIS MODELS FOR TWO MACHINE BUS

The performance equations just presented portray an isolated induction motor. In order to simulate the effects of other motors connected to a common bus during transfer, a representation of at least two interconnected machines is required. To do this, the "circulating current" approach described by Rajamani (8) is used. This is schematically depicted in figure 2.18.

The d-q axis performance equations are combined with current directions observed as shown, that is one machine is assumed to receive current supplied by the other.

When this is done with current flow assumed to be into machine 1, the equation set as shown in Figure 2.19 in matrix form is obtained,

Next the d/dt terms are grouped and the expression becomes as shown in Figure 2.20.

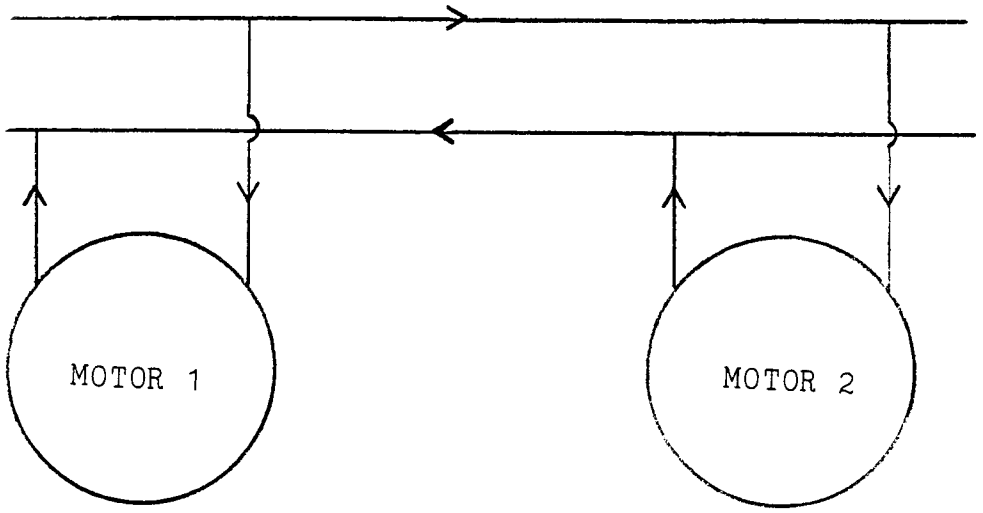


FIGURE 2.18.. CIRCULATING CURRENT APPROACH TO SOLUTION OF INTERCONNECTED INDUCTION MOTOR PROBLEM

	Isd	pIsd	Isq	pIsq	Ird1	pIrd1	Irq1	pIrq1	Ird2	pIrd2	Irq2	pIrq2
0 =	(Rs1 + Rs2)	(Ls1 + Ls2)	-w(Ls1 + Ls2)	0	0	M1	-wM1	0	0	-M2	wM2	0
0 =	w(Ls1 + Ls2)	0	(Rs1 + Rs2)	(Ls1 + Ls2)	wM1	0	0	M1	-wM2	0	0	-M2
0 =	0	M1	-S1M1	0	Rr1	Lr1	-S1Lr1	0	0	0	0	0
0 =	S1M1	0	0	M1	Lr1S1	0	Rr1	Lr1	0	0	0	0
0 =	0	-M2	S2M2	0	0	0	0	0	Rr2	Lr2	-S2Lr2	0
0 =	-S2M2	0	0	-M2	0	0	0	0	S2Lr2	0	Rr2	Lr2

FIGURE 2.19. TWO MOTOR EQUATION SET FOR D-Q MODEL

$$\begin{bmatrix} (Rs1 + Rs2) & -w(ls1 + Ls2) & 0 & -wM1 & 0 & wM1 \\ w(Ls1 + Ls2) & (Rs1 + Rs2) & wM1 & 0 & -wM2 & 0 \\ 0 & -S1M1 & Rr1 & -S1Lr1 & 0 & 0 \\ S1M1 & 0 & S1Lr1 & Rr1 & 0 & 0 \\ 0 & S2M2 & 0 & 0 & Rr2 & -S2Lr2 \\ -S2M2 & 0 & 0 & 0 & S2Lr2 & Rr2 \end{bmatrix} \begin{bmatrix} Isd \\ Isq \\ Ird1 \\ Irq1 \\ Ird2 \\ Irq2 \end{bmatrix}$$

$$+ \begin{bmatrix} (Ls1 + Ls2) & 0 & M1 & 0 & -M2 & 0 \\ 0 & (Ls1 + Ls2) & 0 & M1 & 0 & -M2 \\ M1 & 0 & Lr1 & 0 & 0 & 0 \\ 0 & M1 & 0 & Lr1 & 0 & 0 \\ -M2 & 0 & 0 & 0 & Lr2 & 0 \\ 0 & -M2 & 0 & 0 & 0 & Lr2 \end{bmatrix} \begin{bmatrix} pIsd \\ pIsq \\ pIrd1 \\ pIrq1 \\ pIrd2 \\ pIrq2 \end{bmatrix}$$

FIGURE 2.20 TWO MOTOR EQUATION SET FOR D-Q MODEL WITH D/DT TERMS GROUPED

Which in matrix form can be symbolized as,

$$0 = [H][I] + [G]\, p[I] \qquad (2.35)$$

Manipulating these equations to obtain expressions for differential currents results in,

$$p[I] = -[G]\,\text{inverse}[H][I] \qquad (2.36)$$

Where the matrices are expanded as in Figure 2.21.

The equation sets developed thus far provide the basis for a method of investigating the interaction of motors on a transferred bus. The application of these relationships and the implementation of this method on a digital microcomputer will be described in succeeding chapters.

$$d/dt\ [Isd,\ Isq,\ Ird1,\ Irq1,\ Ird2,\ Irq2] = p\ [I]$$

$$\begin{bmatrix} (Ls1 + Ls2) & 0 & M1 & 0 & -M2 & 0 \\ 0 & (Ls1 + Ls2) & 0 & M1 & 0 & -M2 \\ M1 & 0 & Lr1 & 0 & 0 & 0 \\ 0 & M1 & 0 & Lr1 & 0 & 0 \\ -M2 & 0 & 0 & 0 & Lr2 & 0 \\ 0 & -M2 & 0 & 0 & 0 & Lr2 \end{bmatrix} = [G]$$

$$\begin{bmatrix} (Rs1 + Rs2) & -w(ls1 + Ls2) & 0 & -wM1 & 0 & wM1 \\ w(Ls1 + Ls2) & (Rs1 + Rs2) & wM1 & 0 & -wM2 & 0 \\ 0 & -S1M1 & Rr1 & -S1Lr1 & 0 & 0 \\ S1M1 & 0 & S1Lr1 & Rr1 & 0 & 0 \\ 0 & S2M2 & 0 & 0 & Rr2 & -S2Lr2 \\ -S2M2 & 0 & 0 & 0 & S2Lr2 & Rr2 \end{bmatrix} = [H]$$

FIGURE 2.21 DIFFERENTIAL CURRENT EQUATION SET FOR D-Q MODEL

CHAPTER III

APPLICATION

III.A. PROCEDURE

In order to analyze the response of a particular induction motor during transfer of a bus to which other induction motors are connected, all other motors are consolidated into an equivalent motor. Procedures for performing this have been reported by Watters(10). In essence this involves constructing an equivalent circuit representing a composite motor which matches the composite speed-torque curve of the motors on a bus. The composite speed torque curve is drawn from three weighted points, namely:

a.) full load torque

b.) breakdown torque

c.) starting torque

This lumping of motor parameters is done to reduce computational complexity and thereby remain within the capability of a 48 kilobyte microcomputer without incurring excessive computational time. Each motor of a bus would not need to be examined; only motors with low relative inertias, high viscous damping co-effecients or large loads need close examination.

III.B. PROGRAM DEVELOPMENT

A program in Basic has been written by the author which implements the equation sets described in Chapter II. This program solicits input of induction motor parameters from the conventional equivalent circuits of two machines along with the related mechanical parameters such as inertia and viscous damping. Any load speed torque relationship is readily incorporated. From this data, the steady state operating conditions are computed using the equation set in Figure 2.16.

The program then shifts to the two motor equation set using the "circulating current" approach as shown in Figure 2.18. This analysis assumes that the stator currents instantaneously adjust from steady state values in the first time step. Other researchers such as Ahmed and Abdel-Halem (1) have considered this constraint as reasonable. The program then iteratively computes pI,Te,Wr, Or, motor internal voltage and bus voltage for each time step of a specified bus transfer period.

The angular shift of the rotor of the machine of interest is readily tracked through this interval and problem machine/load combinations are readily identified The resultant volts-per-hertz upon reclosure between system and motor is also computed directly. A flow chart of this program is shown in Figure 3.1.

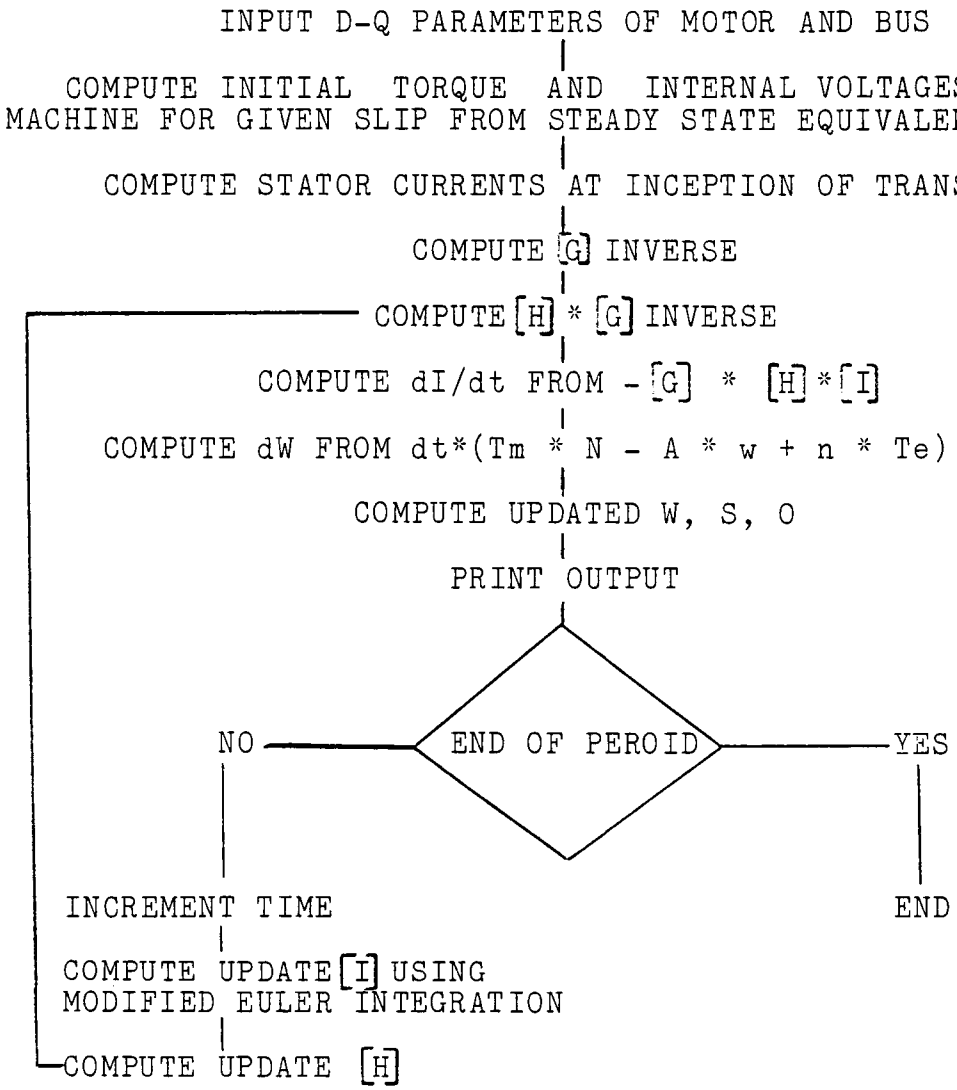


FIGURE 3.1. PROGRAM FLOW CHART

The intergation algorithim chosen for incorporation in this program is the Modified Euler, predictor-corrector. This was selected because it is self-starting and comparitively fast. In investigations thus far, it has shown no signs of instability.

III.C. MOTOR DATA PREPERATION

Previous literature, which has been referenced herein, does not thoroughly treat motor data preparation for use in the d-q axis induction motor equivalent model, in fact some treatments are quite misleading. To dispell any future uncertainty about data preperation, the following motor data tabulation, which has been verified in comparison with conventional equivalent circuit torque computations in steady state, is provided:

CONVENTIONAL MODEL	D-Q SYNCHRONOUS ROTATING MODEL
Rs / PHASE	Rs
Rr / phase	Rr
M / phase	3/2 * M
Ls / phase	Ls + 3/2 * M
Lr / phase	Lr + 3/2 * M
V / phase	$\sqrt{3}$ * V
Te / phase	3 * Te

For machines thus far examined, with machine data from the conventional equivalent circuit adjusted and entered as shown above, the d-q axis model corresponded with the conventional equivalent circuit model within 0.5 percent for steady state performance. Of course no such comparison which is meaningful can be made for transient operation because the conventional equivalent circuit model is not suitable for transient analysis.

III.D. REFERENCE CASE STUDY

As a reference study, two machines with identical electrical and mechanical parameters were examined. The characteristics are:

Ls = .0304 Hy.

Lr = .0304 Hy.

M = .03 Hy.

Rs = .063 Ohm

Rr = .083 Ohm

The operational parameters are:

Initial slip,s, = .003

Viscous damping,A, = .06 Newton-Meters

Inertia,J, = .12 N-M/Kg*Kg

Voltage,V, = 220 V/L-L

This data describes a 30 Horsepower, 4 pole, wye connected motor.

As expected, no power interchange occurred between them and both machines exhibited essentially identical rotor angle opening during power switch off. For this situation, which would be comparable to a single large motor on a bus with aggregate load equivalent to itself, the rotor angle opened 83 degrees during a 6 cycle transfer period and the bus voltage decayed to 63 percent.

This study was done for time steps of .0001 and .001 seconds. Correspondence between these runs was quite close at the end of the six cycle dead bus period, within one degree of rotor swing. Consequently, a time step of .001 was used for subsequent study. Incidentially, in ordinary Basic, this resulted in a computer iteration time of two minutes for each time step which would result in a five hour computer run for a nine cycle bus transfer period. When run in a compiled version, the iteration time for each time step reduced to 15 seconds. Even with this speed up in execution, the computation time for a nine cycle transfer period is approximately twenty minutes. The uncompiled computer memory requirement is 12 kilobytes whereas the compiled version requires 18 kilobytes.

III.E. MOTOR DATA EXAMINATION-CASE I

Motor circuit parameters are obtained as a result of routine tests, often on batches of motors. Consequently characteristics of a particular motor may vary from the particular equivalent circuit data provided for a group of motors of the same rating. The sensitivity of the aforementioned model to imprecise data required examination to establish the needed precision of motor parameters.

Each electrical and mechanical parameter in the performance equations of the motor being examined was increased by 20 percent in turn with all other parameters held at the reference level for a nine cycle transfer period. This was repeated for 20 percent decrease of each parameter of the motor in turn.

The results of these computer runs for these machine data variances are summarized in Table 3.1 for volts/hertz ratio and relative rotor flux angle at the end of a nine cycle (.15 second) period of bus de-energization. From this data examination, it is apparent that a +/- 20 percent varaition in data did not appreciably affect results for mutual inductances, stator inductances, rotor inductances, stator resistances or viscous damping coeffecients.

TABLE 3.1. TABULATION OF RESULT DEVIATIONS DUE TO +/- 20 PERCENT DATA DEVIATIONS AFTER NINE CYCLES FOR CASE I

PARAMETER	VOLTS/HERTZ RATIO	ROTOR ANGLE
Ls * 0.8	1.534	195.1
Ls * 1.2	1.534	194.1
Lr * 0.8	1.533	194.6
Lr * 1.2	1.535	194.6
M * 0.8	1.507	194.0
M * 1.2	1.552	195.0
Rr * 0.8	1.481	217.1
Rr * 1.2	1.535	179.0
Rs * 0.8	1.534	194.7
Rs * 1.2	1.534	194.6
J * 0.8	1.464	215.8
J * 1.2	1.557	177.4
A * 0.8	1.535	194.1
A * 1.2	1.533	195.2

The variation of results due to a +/- 20 percent change in inertia and rotor resistance is, however, noticeable. The data for the computer runs with +/- 20 percent inertia is presented in Table 3.2 and plotted in Figure 3.2. In the area of interest, 1.33 volts/hertz, note that an uncertainty of +/- 20 percent in inertia yields a corresponding uncertainty of +/- 0.5 percent in volts/hertz ratio. This plot reveals that a safe bus transfer can be done in the region of six cycles (0.1 seconds).

This plot also illustrates the effect of rotor flux phase angle quite well. The turndown of volts/hertz ratio after 0.13 seconds corresponds with the rotor flux angle increasing beyond 180 degrees. Thus the rotor flux is dropping back toward an in-phase position with relation to the system flux.

The other parameter variation which noticeably influenced these results was rotor resistance. The data for this is presented in Table 3.3 and plotted in Figure 3.3. At the reqion of interest, that is 1.33 volts/hertz, a +/- 20 percent rotor resistance uncertainty results in a +/- 0.07 uncertainty in volts/hertz ratio.

Other parameter variations of +/- 20 percent did not cause result deviations greater than 0.01 for volts/hertz ratio nor more than one degree of rotor swing.

TABLE 3.2. TABULATION OF EFFECT OF +/- 20 PERCENT INERTIA ON CASE I

	+20 PERCENT J		-20 PERCENT J	
TIME	VOLTS/HERTZ	ANGLE	VOLTS/HERTZ	ANGLE
.01	.053	1.4	.057	1.7
.02	.110	4.4	.126	5.6
.03	.186	9.0	.217	11.2
.04	.281	15.0	.331	18.4
.05	.395	22.5	.469	27.6
.06	.526	31.6	.635	38.7
.07	.671	42.1	.794	51.5
.08	.824	54.1	.969	66.1
.09	.980	67.5	1.140	82.4
.10	1.134	82.3	1.300	100.4
.11	1.276	98.5	1.432	120.1
.12	1.400	116.2	1.527	141.6
.13	1.493	135.2	1.571	164.7
.14	1.549	155.6	1.552	189.4
.15	1.557	177.4	1.464	215.8

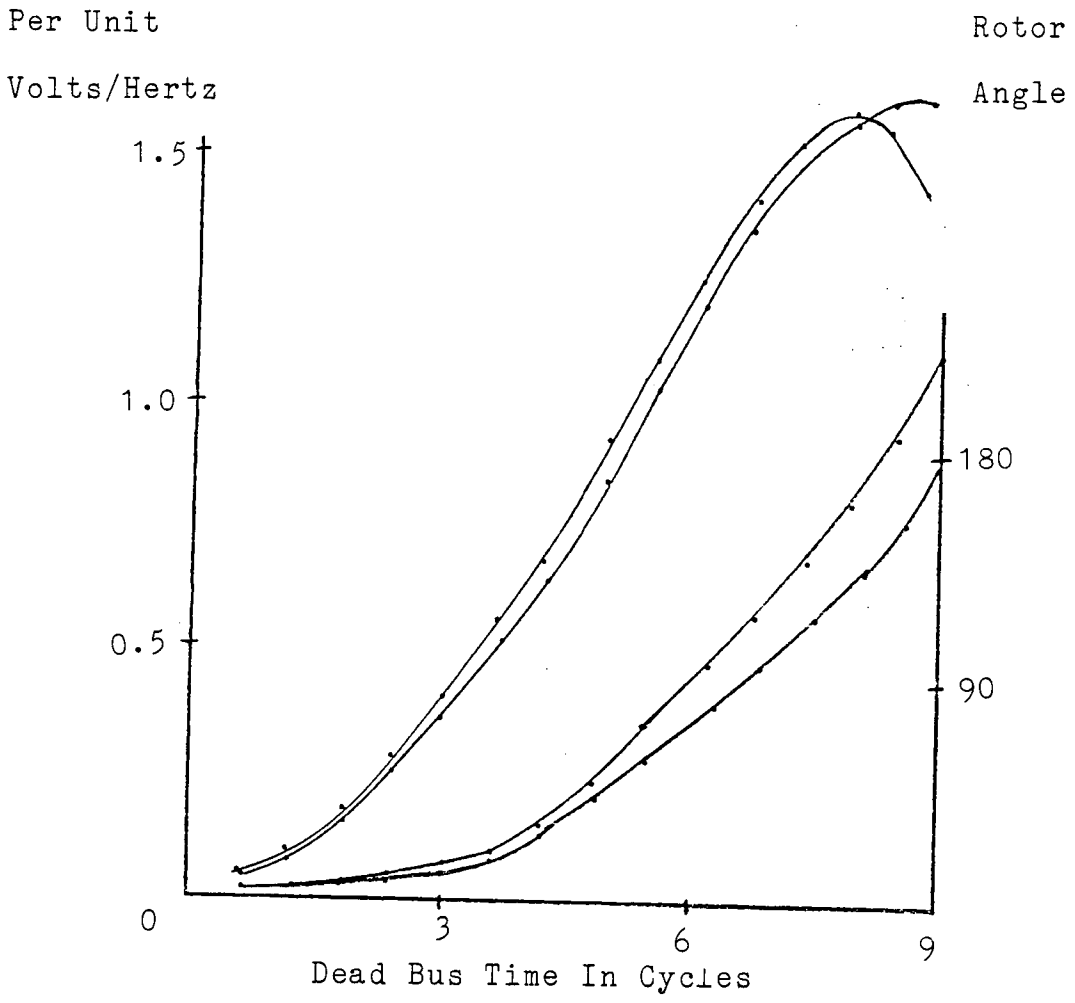


FIGURE 3.2. PLOT OF EFFECT OF +/- 20 PERCENT INERTIA ON CASE I

TABLE 3.3. TABULATION OF EFFECT OF +/- 20 PERCENT ROTOR RESISTANCE ON CASE I

	+20 PERCENT Rr		-20 PERCENT Rr	
TIME	VOLTS/HERTZ	ANGLE	VOLTS/HERTZ	ANGLE
.01	.056	1.4	.054	1.7
.02	.115	4.5	.122	5.6
.03	.191	9.0	.214	11.2
.04	.287	15.1	.330	18.6
.05	.401	22.7	.470	27.8
.06	.531	31.8	.629	38.9
.07	.675	42.4	.802	51.9
.08	.826	54.5	.981	66.5
.09	.981	68.0	1.156	82.9
.10	1.132	83.0	1.319	101.1
.11	1.271	99.4	1.455	121.0
.12	1.391	117.2	1.552	142.5
.13	1.481	136.5	1.596	165.7
.14	1.531	157.1	1.575	190.6
.15	1.535	179.1	1.481	217.1

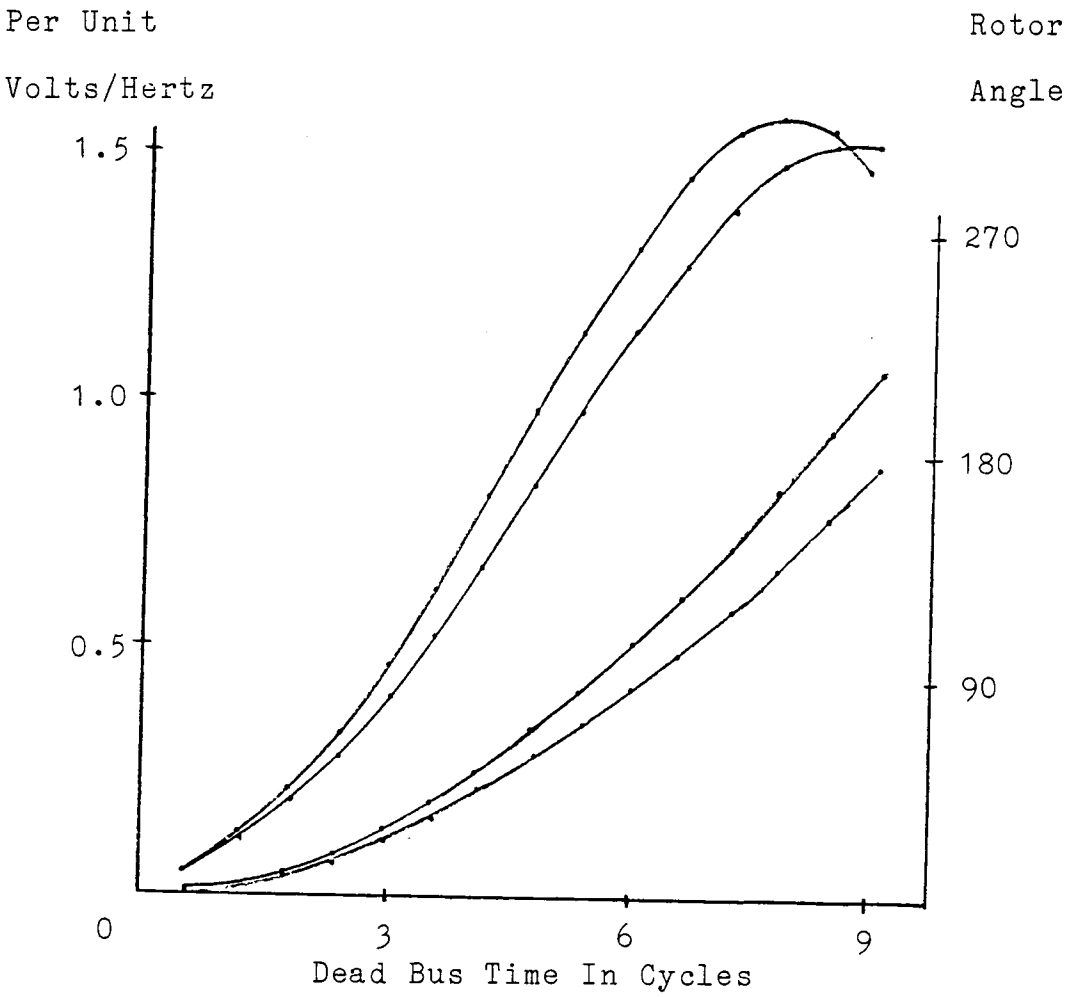


FIGURE 3.3. PLOT OF EFFECT OF +/- 20 PERCENT ROTOR RESISTANCE ON CASE I

Consequently, neither data tabulations nor curve plotting present meaningful data and therefore they are not listed.

III.F. MOTOR DATA EXAMINATION - CASE II

An additional case study was done for a small motor connected to a bus. The data for this study represents a three horsepower motor connected to an aggregate bus of 30 horesepower. Essential motor characteristics are:

Ls = 0.206 henry

Lr = 0.206 henry

M = 0.200 henry

Rs = 0.140 ohm

Rr = 0.110 ohm

A = 0.03 newton-meters

J = 0.03 newton-meters/kilogram squared

V = 220 volts line to line

The results of these computer runs for machine data variances of +/- 20 percent are presented in Table 3.4. Here again the effect of +/- 20 percent variance in viscous damping coeffecient, rotor inductance, stator inductance, mutual inductance and stator resistance was negligible. A difference of less that 0.02 in volts/hertz ratio and less than three degrees in rotor flux position existed at the end of a nine cycle de-energized period.

TABLE 3.4. TABULATION OF RESULT DEVIATIONS DUE TO +/- 20 PERCENT DATA DEVIATIONS AFTER NINE CYCLES FOR CASE II

PARAMETER	VOLTS/HERTZ RATIO	ROTOR ANGLE
Ls * 0.8	1.162	269.0
Ls * 1.2	1.189	266.2
Lr * 0.8	1.176	267.6
Lr * 1.2	1.175	267.6
M * 0.8	1.185	266.2
M * 1.2	1.169	268.6
Rr * 0.8	0.950	291.6
Rr * 1.2	1.313	250.9
Rs * 0.8	1.175	267.7
Rs * 1.2	1.176	267.6
J * 0.8	1.069	279.1
J * 1.2	1.269	256.9
A * 0.8	1.182	266.9
A * 1.2	1.170	268.3

Noticeable variations in results for inertia and rotor resistance variances of +/- 20 percent did occur. The inertia data is presented in Table 3.5 and plotted in Figure 3.4. Rotor resistance variation results are presented in Table 3.6 and plotted in Figure 3.5.

Here again, in the region of 1.33 volts/hertz, uncertainties of +/- 20 percent in these parameters resulted in volts/hertz ratio uncertainties of +/- 0.05 for inertia variances and 0.07 for rotor resistance variances.

TABLE 3.5. TABULATION OF EFFECT OF +/- 20 PERCENT INERTIA ON CASE II

	+20 PERCENT J		-20 PERCENT J	
TIME	VOLTS/HERTZ	ANGLE	VOLTS/HERTZ	ANGLE
.01	.056	1.9	.064	2.5
.02	.124	6.1	.152	7.9
.03	.235	13.0	.284	16.1
.04	.383	22.4	.444	26.3
.05	.558	33.9	.622	38.2
.06	.749	47.3	.815	52.0
.07	.950	62.5	1.020	68.2
.08	1.150	79.6	1.227	87.0
.09	1.337	98.7	1.417	108.3
.10	1.498	119.9	1.565	132.0
.11	1.613	143.3	1.650	157.6
.12	1.661	168.9	1.651	185.0
.13	1.626	196.4	1.556	214.3
.14	1.269	225.7	1.359	245.6
.15	1.269	256.9	1.069	279.1

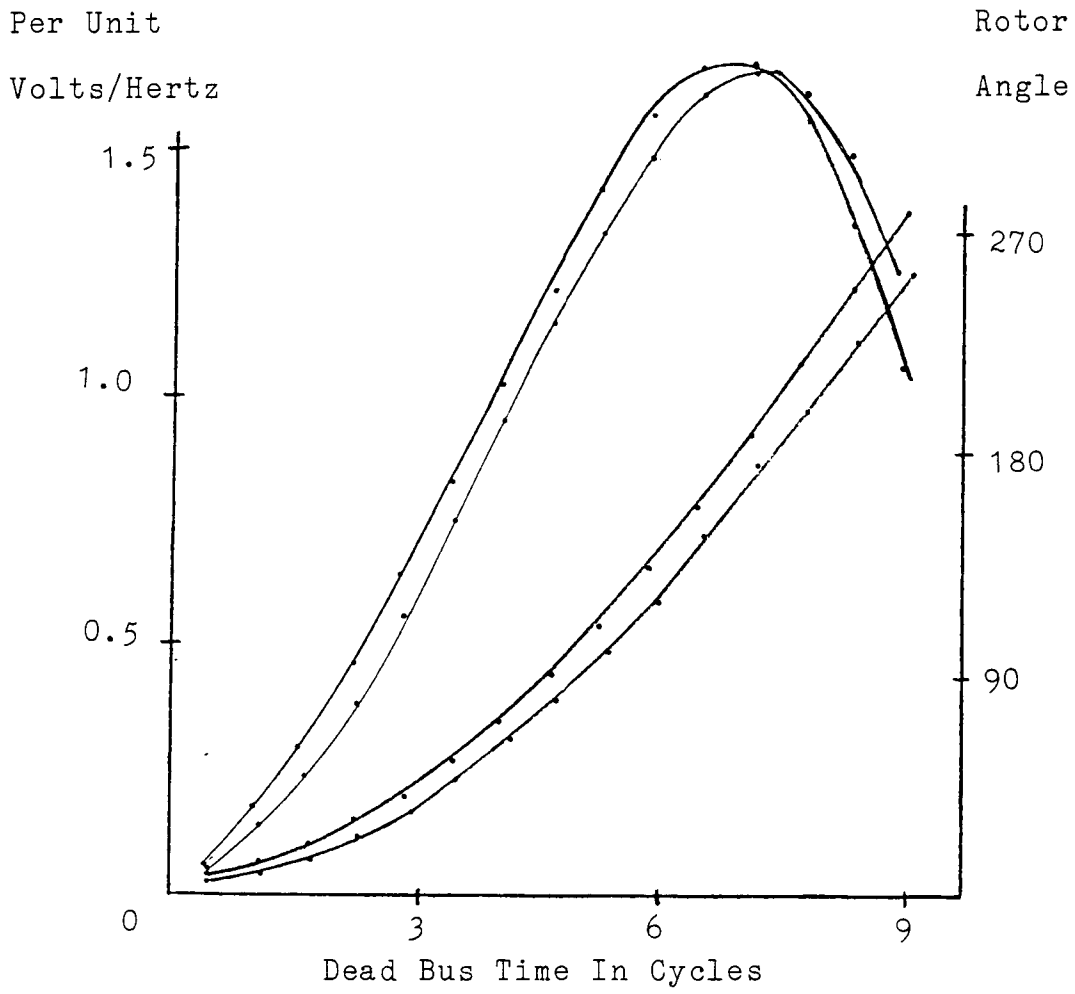


FIGURE 3.4. PLOT OF EFFECT OF +/- 20 PERCENT INERTIA ON CASE II

TABLE 3.6. TABULATION OF EFFECT OF +/- 20 PERCENT ROTOR RESISTANCE ON CASE II

	+20 PERCENT Rr		-20 PERCENT Rr	
TIME	VOLTS/HERTZ	ANGLE	VOLTS/HERTZ	ANGLE
.01	.054	1.9	.067	2.6
.02	.124	6.1	.154	8.0
.03	.235	13.0	.289	16.4
.04	.381	22.2	.457	27.2
.05	.550	33.4	.646	39.9
.06	.735	46.3	.849	54.6
.07	.929	60.9	1.060	71.5
.08	1.124	77.5	1.268	90.8
.09	1.312	96.3	1.454	112.9
.10	1.474	117.2	1.595	137.4
.11	1.594	140.2	1.664	164.2
.12	1.651	165.2	1.641	193.1
.13	1.629	192.0	1.511	224.0
.14	1.517	220.6	1.275	256.8
.15	1.313	250.9	.950	291.6

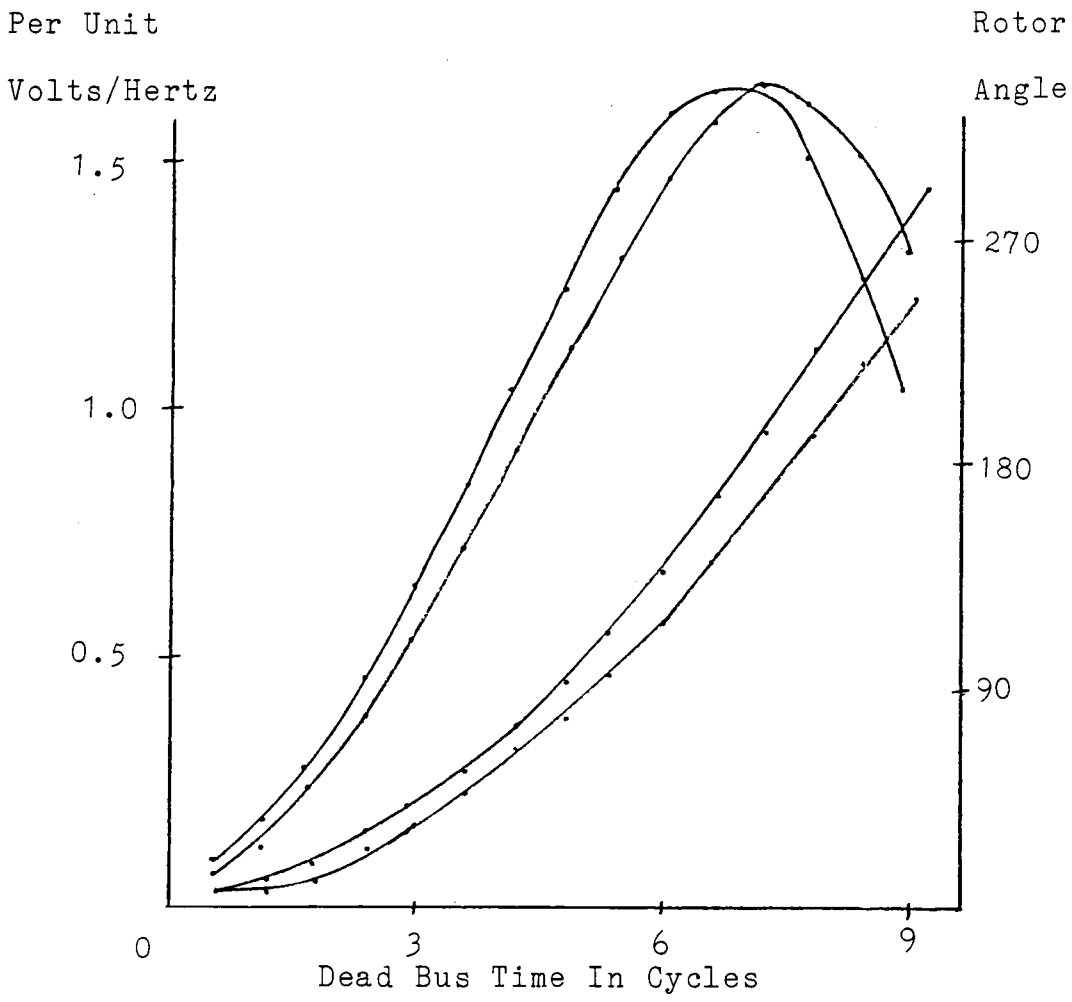


FIGURE 3.5. PLOT OF EFFECT OF +/- 20 PERCENT ROTOR RESISTANCE ON CASE II

CHAPTER IV

CONCLUSION

In order to determine the severity of a bus transfer on a motor, a digitial computer program has been developed which utilizes the d-q model of an induction motor on synchronously revolving reference axes. Two such models are interconnected in the program representation to enable representation of a particular motor and a composite of interconnected motors on the same bus.

Conversion of data from the conventional equivalent circuit model into a form suitable for the d-q axis model has been presented.

The sensitivity of this motor bus representation to motor parameter variation has been investigated to assess the impact of imprecise data on calculated rotor angle swing. For one case investigated with the motor of interest of equal size to the equivalent bus, conventional circuit data deviation of 20 percent did not introduce rotor swing changes of more than 39 degrees during a nine cycle bus transfer period. Resultant volts-per-hertz ratio deviations upon reclosure did not exceed 0.09. A second case investigated featured a motor of one tenth the size of the equivalent bus. Here, the conventional circuit data deviation of 20 percent resulted in a maximum resultant volts/hertz ratio deviation of 0.36 and a rotor

swing deviation of 40 degrees at the end of nine cycles of dead bus time.

Certainly, situations may exist where sensitivity is much increased, however it has not been the intent of this investigation to identify these instances, rather the intent of this study has been to develop the tool whereby they may be readily discovered.

This analysis tool has been developed such that it will run on a 48 kilobyte microcomputer and has been coded in Basic. As such it is readily useable by auxiliary power system designers to investigate the potential severity of bus transfers on a particular motor without resorting to expensive central computers and lends itself to adaptation to a spectrum of needs.

The expectation is that such an analysis tool will find wide application in auxiliary power system design studies to check motor bus transfer characteristics and also investigate the sensitivity of particular combinations of motors to deviations in motor data, which inevitably occur. The author expects to utilize this tool in examining response of induction motors during fast bus transfers at installations designed by his employer, the Tennessee Valley Authority, Division of Engineering Design, Knoxville, Tennessee. This will enable critical bus transfer times to be identified for particular motors with confidence not heretofore possible.

LIST OF REFERENCES

LIST OF REFERENCES

1) Ahmed, Farouk I., and I. A. M. Abdel-Hasim:"Exact Analytical Solution Of Induction Motor Equations Following Supply Disconnection," Electric Machines and Electromechanics, No. 5, pp 323-330

2) Daugherty, R. H. :"Analysis Of Transient Electrical Torques And Shaft Torques in Induction Motors As A Result Of Power Supply Distrubances,"IEEE Transactions on Power Apparatus and Systems, Vol. PAS-101, No. 8, August, 1982, pp 2826-2836

3) De Sakar, Asish K., and Gunnar J. Berg:"Digitial Simulation of Three-Phase Induction Motors,"IEEE Transactions on Power Apparatus and Systems, Vol. PAS-89, No. 6, July/August 1970, pp 1031-1037

4) Fink, D. G., and H. W. Beaty: "Strandard Handbook for Electrical Engineers," 11th. ed., McGraw-Hill, Inc., New York, 1978

5) Krause, Paul C.: "Method of Multiple Reference Frames Applied To The Analysis of Symmetrical Induction Machinery," IEEE Transactions on Power Apparatus and Systems, Vol. PAS-87, No. 1, January 1968, pp 218-227

6) Nasar, S. A., and L. E. Unneweher: "Electromechanics and Electric Machines, "1st ed., John Wiley & Sons, Inc., New York, 1979

7) O'Kelley, D. O., and S. Simmons: "Introduction to Generalized Electrical Machine Theory," 1st. ed., McGraw-Hill Publishing Company Limited, London, 1968

8) Rajamani, K. :"Report On Analysis Of Dynamic Performance Of Induction Motors," TATA Consulting Engineers, Bombay

9) Sastry, K. P. R., and R. E. Burridge: "Investigation of a Reduced Order Model For Induction Machine Dynamic Studies,"IEEE Transactions on Power Apparatus and Systems, Vol. PAS-95, No. 3, May/June 1976, pp 962-969

10) Watters, C. V. :"A Simplified Procedure for Determining The Auxiliary Bus Voltage And Angle During Bus Transfer," IEEE Transactions on Power Apparatus and Systems, Vol. PAS-100, No. 6, June 1981, pp 3066-3076

VITA

John Kenneth Greene was born in Maringouin, Louisiana, on February 28, 1943. He attended elementary school in Fenton, Louisiana, and was graduated from Fenton High School in 1961.

He then entered Louisiana State University in Baton Rouge, Louisiana, in June 1961 and received the Bachelor of Science degree in electrical engineering in January 1966. During this period he was employed at a number of radio and television stations as transmitter engineer, having obtained a Federal Communications Commission First Class Radio Operators License in 1960.

Following graduation, he was then employed by the Los Angeles Department of Water and Power in the inspecting, testing and contract enforcement for electrical power system equipment until 1974. Assignments included Japan (2 years), Europe (2 years) and eastern US (5 years) involving direct current high voltage equipment, transformers and circuit breakers to 500 kv and associated electrical hardware.

He has been employed by the Tennessee Valley Authority, Knoxville, Tennessee, in the Division of Engineering Design's Electrical Engineering Branch since January 1974. He is presently a senior electrical

engineer in charge of the Heavy Electrical Equipment Contract Engineering Section.

He received the Tennessee professional engineers license in 1979 and the degree of Master of Science in electrical engineering from The University of Tennessee, Knoxville in June 1983.